

Supporting information

Aerobic oxidative dehydrogenation of N-heterocycles over OMS-2-based nanocomposite catalyst: preparation, characterization and kinetic study

Xiuru Bi,^{a,b} Tao Tang,^{a,b} Xu Meng,^{a,*} Mingxia Gou,^a Xiang Liu,^{c,*} Peiqing Zhao^{a,*}

^a State Key Laboratory for Oxo Synthesis and Selective Oxidation, Suzhou Research Institute of LICP, Lanzhou Institute of Chemical Physics (LICP), Chinese Academy of Sciences, Lanzhou 730000, China. Fax: + 96 931 8277008, Tel: + 86 931 4968688, E-mail: xumeng@licp.cas.cn, zhaopq@licp.cas.cn

^b University of Chinese Academy of Sciences, Beijing 100049, China.

^c College of Materials and Chemical Engineering, Key Laboratory of Inorganic Nonmetallic Crystalline and Energy Conversion Materials, China Three Gorges University, Yichang, Hubei 443002, China. E-mail: xiang.liu@ctgu.edu.cn

CONTENTS

1. General Information	2
2. Synthesis raw	2
3. Catalytic activity comparison of 2[PW]-OMS-2 with other reported catalytic systems	2
4. Recycling experiment of 2 [PW]-OMS-2 and catalyst characterization	3
5. Kinetic study	6
6. Discussion of the reaction mechanism	7
7. Reference	9
8. Spectrum data of the products	9
9. Copies of ¹ H and ¹³ C Spectra	17-46

1. General Information

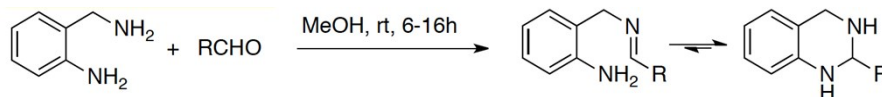
All reagents were purchased from commercial suppliers and used without further purification and DMC (CAS NO. 616-38-6, ReagentPlus®, 99%) was purchased from Sigma-Aldrich with a mark of Greener Alternative Product. All experiments were carried out under air or using O₂/N₂ balloon. Flash chromatography was carried out with Merck silica gel 60 (200-300 mesh). Analytical TLC was performed with Merck silica gel 60 F254 plates, and the products were visualized by UV detection. ¹H NMR and ¹³C NMR (400 and 100 MHz respectively) spectra were recorded in CDCl₃. Chemical shifts (δ) are reported in ppm using TMS as internal standard, and spin-spin coupling constants (J) are given in Hz.

2. Synthesis of raw

3.1 The procedure of synthesis of substituted 1,2,3,4-tetra-hydroquinoline **1h** and **1i**^[1]

Benzylic azide (2.33 mmol) was dissolved in CH₂Cl₂ (15 mL) and cooled to 0 °C. TfOH (2.83 mmol) was added and the solution was allowed to stir for 10 min at r. t. The corresponding styrene (14.68 mmol) was then added and the reaction was stirred at 0 °C until completion. The reaction was quenched by addition of saturated aqueous Na₂CO₃ and extracted into EtOAc (3 x 100 mL). The organic phase was washed with brine, dried over MgSO₄, concentrated and purified by column chromatography.

3.2 The procedure of synthesis of 1,2,3,4-tetrahydroquinazoline derivatives **3a-3g**^[2]



2-amino-benzyl amine (17.8 mmol) was dissolved in MeOH (100 mL) and the corresponding aldehyde (17.8 mmol) was added. The reaction mixture was stirred at r.t. for 20 h. The formed solid was filtrated, washed by EtOH and dried to offer the desired tetrahydroquinazolines **3a-3g**.

3.3 The procedure of synthesis of Hantzsch esters **3n-3q**^[3]

Aqueous solution of ammonia (10 mL, 25 wt%), the corresponding aldehyde (0.1 mol) and carbonyl acid ester (0.2 mol) were mixed and stirred for 12 h at r. t. under air. Cool water was added into the mixture and yellow precipitate was formed. Yellow solid was collected by filtration and dried to afford Hantzsch esters.

3. Catalytic activity comparison of 2[PW]-OMS-2 with other reported catalytic systems.

Table S1. Catalytic activity comparison of 2[PW]-OMS-2 with other reported catalytic systems.

Entry	Catalyst	Oxidant	Temp. (°C)	Con. (%)	Sel. (%)
1	2[PW]-OMS-2	O ₂ , 1atm	80 °C	>99	99
2 ^[4]	Co@NGS-700	O ₂ , 1atm	80 °C	62	96
3 ^[4]	Co@C	O ₂ , 1atm	80 °C	14	38
4 ^[4]	NGs	O ₂ , 1atm	80 °C	13	31
5 ^[4]	Co/NAC	O ₂ , 1atm	80 °C	43	35
6 ^[5]	FeOx@NGr-C	O ₂ , 1atm	80 °C	100	83
7 ^[6]	NiMn ₂ -LDH	O ₂ , 1atm	100 °C	>99	86
8 ^[7]	Pd/SiO ₂	Air, 1atm	180 °C	99	75
9 ^[8]	Co-N-C (0.5mol%)	O ₂ , 1atm	125 °C	87	100
10 ^[9]	Co ₃ O ₄ -NGr/C	O ₂ , 1atm	60 °C	100	90

4. Recycling experiment of 2 [PW]-OMS-2 and catalyst characterization

Firstly, the catalytic reaction proceeded smoothly when the reaction scale was increased to 10 mmol of **1a** with 1 g of 2 [PW]-OMS-2 in 50 mL of DMC. When the reaction was finished, the solid catalyst was isolated by centrifugation and washed by a large amount of EtOH. After that, the catalyst was dried in oven at 60 °C overnight.

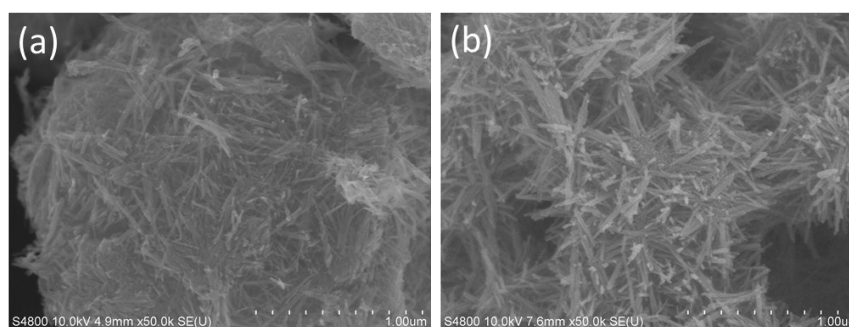


Fig. S1. The TEM images of 2 [PW]-OMS-2.

As shown in the Figure S1, the 2 [PW]-OMS-2 has a typical and uniform nanorod morphology, which means that W-doping does not change the structure and morphology of OMS-2.

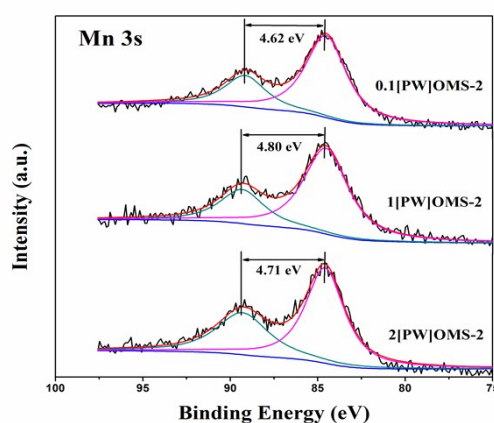


Fig. S2. XPS patterns of as-synthesized materials.

Through the analysis of Mn 3s XPS spectra, average oxidation state (AOS) of Mn was calculated based on the following formula: $AOS = 8.956 - 1.126 \times \Delta E$, where ΔE is the binding energy difference between the doublet Mn 3s peaks as shown in Fig. S2. The ΔE value of 0.1 [PW]-OMS-2, 1 [PW]-OMS-2, and 2 [PW]-OMS-2 is 4.62 eV, 4.80 eV, and 4.71 eV, respectively.

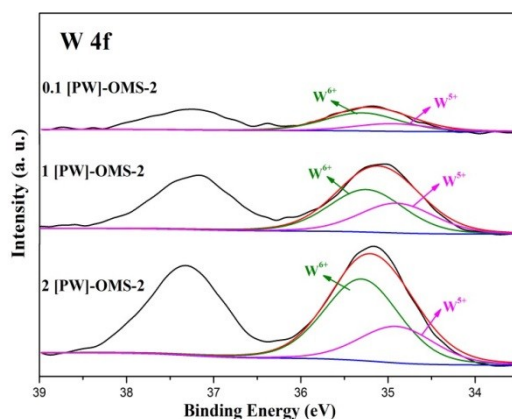


Fig. S3. The W 4f XPS patterns of as-synthesized materials.

Table S2. The W 4f XPS of as-synthesized materials.

Catalyst	Binding energy of W 4f (eV)		Tungsten species (%)	
	W ⁶⁺	W ⁵⁺	W ⁶⁺	W ⁵⁺
0.1 [PW]-OMS-2	35.30	34.95	70.4	29.6
1 [PW]-OMS-2	35.25	34.92	58.8	41.2
2 [PW]-OMS-2	35.30	34.95	69.1	30.9

The W 4f XPS spectra of 0.1 [PW]-OMS-2, 1 [PW]-OMS-2 and 2 [PW]-OMS-2 are shown in Figure. S3. The W 4f spectra could be fitted into two peaks, the lower binding energy was assigned to W⁵⁺ and the higher to W⁶⁺. As shown in Table S2, the content of W⁵⁺ and W⁶⁺ were calculated by their peak areas respectively. The results show that the content of W⁶⁺ is higher among 0.1 [PW]-OMS-2, 1 [PW]-OMS-2 and 2 [PW]-OMS-2. Among them, W⁶⁺ accounts for 69.1% in 2 [PW]-OMS-2.

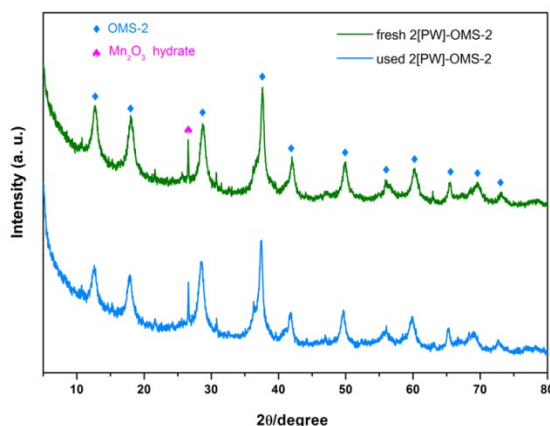


Fig. S4. The XRD patterns of fresh 2 [PW]-OMS-2 and 2 [PW]-OMS-2 reuse for 10 times.

The change of retrieved catalyst was measured by XRD, which confirms that cryptomelane/ Mn_2O_3 hydrate phases and crystallinity were retained after five recycles.

Table S3. The BET properties of fresh [PW]-OMS-2 and recovery 2 [PW]-OMS-2 catalysts.

Catalyst	Surface area ($\text{m}^2 \text{g}^{-1}$)	Pore volume ($\text{cm}^3 \text{g}^{-1}$)	Pore size (nm)
2 [PW]-OMS-2	204	0.59	13
Recovery 2 [PW]-OMS-2	202	0.57	14

N_2 adsorption/desorption measurement was performed to explore the change of the textural parameters of used 2 [PW]-OMS-2. The S_{BET} , pore volume, and average pore diameter all maintained after five recycles, suggesting that 2 [PW]-OMS-2 has good structural stability.

Table S4. Optimization of the amount of catalyst under standard conditions ^a.

No.	1	2	3	4	5	6
Catalyst (mg)	5	10	15	20	25	30
Yield(%) ^b	42	67	84	98	98	98

^a Reaction conditions: 1,2,3,4-tetrahydroquinoline (0.2 mmol), 2 [PW]-OMS-2, DMC (1 mL), O_2 balloon, 80°C , 6

h. ^b Yields were determined by GC.

In the Table S4, the amount of catalyst was optimized under the standard conditions. When 20 mg of 2 [PW]-OMS-2 was used for 0.2 mmol of substrate, the highest yield of **2a** was obtained. Further increasing the amount of catalyst did not increase the yield and conversion of the reaction.

5. Kinetic study

4.1 Calculation of Weisz-Prater Criterion^[10]

D_{eff} = effective diffusivity of a reactant "A", cm²/s

$$D_{eff} = D_{b,A} \frac{(1 - \lambda)^2}{1 + P\lambda}$$

Where

$D_{b,A}$ = the diffusivity of a reactant "A" in the bulk phase, cm²/s; calculated by Wilke-Chang method.^[11]

λ = the ratio of the radius of the diffusing molecule to the pore radius

P = a fitting parameter, estimated according to ref. 10.

$$\Phi_{WP/O_2} = \frac{\left(2.336 * 10^{-3} \frac{mol}{cm^{-3}.s}\right) (0.65 * 10^{-6} cm)^2}{\left(7.9 * 10^{-6} \frac{mol}{cm^3}\right) \left(1.11 * 10^{-4} \frac{cm^2}{s}\right)} = 1.125 * 10^{-4}$$

$$\Phi_{WP/tetrahydroquinoline} = \frac{\left(2.336 * 10^{-3} * \frac{mol}{cm^3.s}\right) (0.65 * 10^{-6} cm)^2}{\left(1 * 10^{-3} \frac{mol}{cm^3}\right) \left(3.28 * 10^{-6} \frac{cm^2}{s}\right)} = 3.009 * 10^{-4}$$

4.2 Initial rates with respect to the amount of substrate (1a)

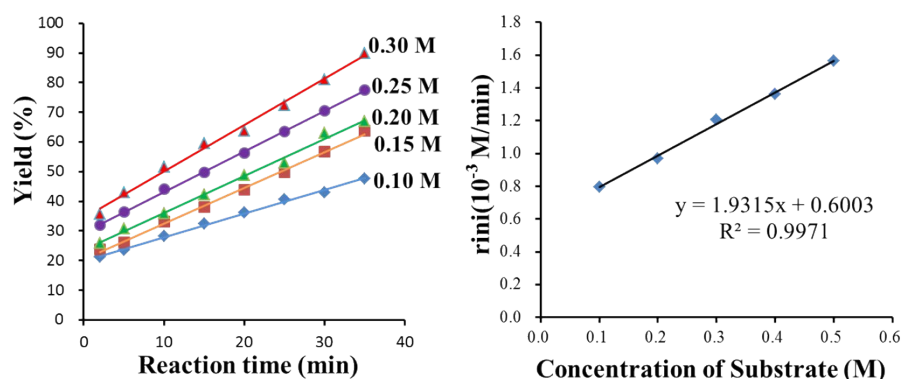


Fig. S5. Initial rates with respect to substrate (1a).

As shown in Fig.S5, in the dehydrogenation system of 1,2,3,4-tetrahydroquinoline to quinoline, the initial reaction rate increases with the increasing concentration of substrate **2a**, showing a good linear relationship. The results indicated that the dehydrogenation of 1,2,3,4-tetrahydroquinoline is a first-order reaction, consistent with the result for mesoporous manganese oxide catalyst.^[13]

4.3 Initial rates with respect to the amount of catalyst

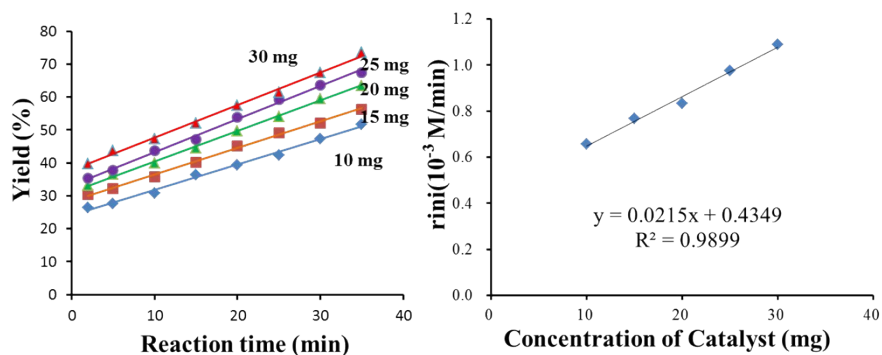


Fig. S6. Initial rates with respect to catalyst.

As shown in Fig. S6, in the dehydrogenation system of 1,2,3,4-tetrahydroquinoline to quinoline, the initial reaction rate increases with the increasing concentration of catalyst, showing a good linear relationship. The results indicated that the dehydrogenation of 1,2,3,4-tetrahydroquinoline is a first-order reaction, consistent with the result for mesoporous manganese oxide catalyst.^[13]

5.4 Initial rates with respect to temperature

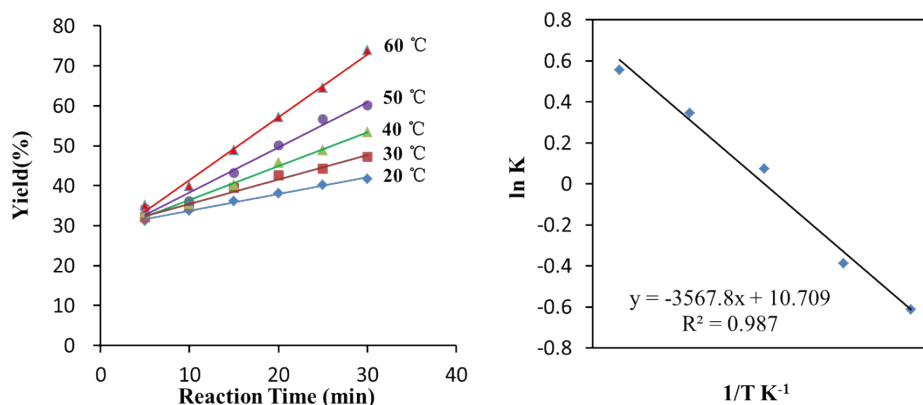
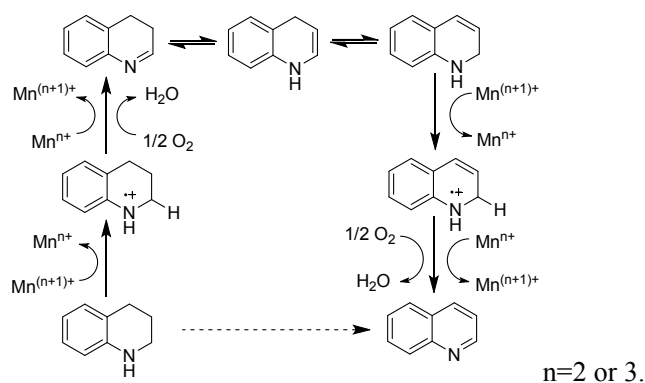


Fig. S7. First-order kinetics fit and Arrhenius plot of dehydrogenation of 1,2,3,4-tetrahydroquinoline. Reaction conditions: 1,2,3,4-tetrahydroquinoline 0.2 mmol, 2 [PW]-OMS-2 20 mg, DMC 2 mL, under oxygen.

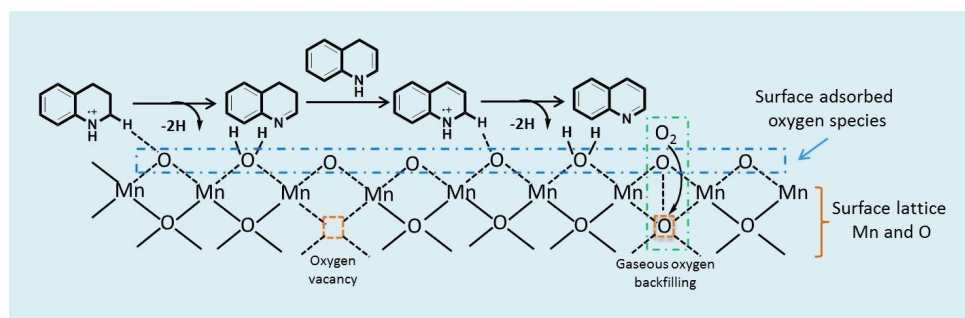
As shown in Fig. S7., in the dehydrogenation system of 1,2,3,4-tetrahydroquinoline to quinoline, the initial reaction rate increases with the temperature increasing. A multiple regression analysis for the constants in Fig. S7. against temperature with this expression led to a value of 29.66 kJ•mol⁻¹ for the apparent activation energy (Ea).

6. Discussion of the reaction mechanism

A possible reaction mechanism for the aerobic oxidation dehydrogenation of 1,2,3,4-tetrahydroquinoline under 2 [PW]-OMS-2.



Scheme S1. Proposed mechanism of oxidative aromatization of 1,2,3,4-tetrahydroquinoline.



Scheme S2. The probable mechanisms of 1,2,3,4-tetrahydroquinoline adsorption and oxidation over 2 [PW]-OMS-2.

The transfer of electron of nitrogen in saturated cycloalkane to the catalyst metal Mn center is a necessary for the initiation of the reaction. Then, the formed amine radical species can be subjected to a C–H dehydrogenation to form an imine intermediate (Scheme S1). The experimental results verified the above proposed mechanism that the substrate lacking a C-H proton does not form any dehydrogenation product. Thereafter, the imine of the primary dehydrogenation product is subjected to tautomeric cyclic imine and through the secondary dehydrogenation to obtain the final dehydrogenation product.^[14] The formation of the radical amine intermediate results in a decrease of the surface active Mn center, which results in the release of labile lattice oxygen.^[15,16] During the process, the aerobic atmosphere is necessary as the lattice oxygen requires the oxygen in the atmosphere to replenish. The above proposed mechanism is consistent with the observation that the catalytic efficiency is low under N₂ (32 % yield) compared to aerobic conditions (98% yield). After 32% yield was obtained, the substrate was no further conversion, which probably due to the reduced Mn species was not completely re-oxidized because the lack of oxygen.

The probable mechanisms of 1,2,3,4-tetrahydroquinoline adsorption and oxidation over 2 [PW]-OMS-2. 1,2,3,4-tetrahydroquinoline is adsorbed onto the surface initially via the

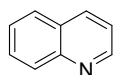
interaction between the C-H proton and surface adsorbed oxygen species. After a one-step dehydrogenation to form the imine of the primary dehydrogenation product, it is subjected to tautomeric cyclic imine and through the secondary dehydrogenation to obtain the final dehydrogenation product. During this process, imine is adsorbed onto surface in the same way. When two H atoms and one surface adsorbed oxygen atom leave the reaction interface as H₂O, the oxygen vacancy can introduce oxygen atoms from the oxygen to renewal of the missing lattice oxygen in the catalyst. Thus, the stable structure and excellent catalytic activity of the catalyst are maintained well. Therefore, the labile lattice oxygen and oxygen vacancies play a vital role in the formation of quinoline^[17].

7. Reference

- [1] W. H. Pearson, W.-K. Fang, *Israel J. Chem.* 37 (1997) 39-46.
- [2] A. E. Wendlandt, S. S. Stahl, *J. Am. Chem. Soc.* 136 (2014) 11910-11913.
- [3] A. Kumar, R. A. Maurya, *Synlett.* 6 (2008) 883-885.
- [4] J. Li, G. Liu, X. Long, G. Gao, J. Wu, F. Li, *J. Catal.* 355 (2017) 53-62.
- [5] M. Beller, *J. Am. Chem. Soc.* 137 (2015) 10652-10658.
- [6] W. Zhou, Q. Tao, F. Sun, X. Cao, J. Qian, J. Xu, M. He, Q. Chen, J. Xiao, *J. Catal.* 361 (2018) 1-11.
- [7] J. Zhang, D. Li, G. Lu, T. Deng, C. Cai, *ChemCatChem*, 10(2018)4966- 4972.
- [8] S. Nie, J. Wang, X. Huang, X. Niu, L. Zhu, X. Yao, *ACS Appl. Nano Mater.* 1(2018) 6567-6574.
- [9] A. V. Iosub, S. S. Stahl, *Org. Lett.*, 17(2015) 4404-4407.
- [10] S. Mukherjee, M.A.Vannice, *J. Catal.* 243 (2006) 108-130.
- [11] C.R. Wilke, P. Chang, *AIChE J.* 1 (1995) 264-270.
- [12] M. Ternan, *J. Can. Chem. Eng.* 65 (1987) 244-249.
- [13] K. Mullick, S. Biswas, A.M. Angeles-Boza, S.L. Suib, *Chem. Commun.* 53 (2017) 2256-2259.
- [14] S. Chakraborty, W. W. Brennessel, W. D. Jones, *J. Am. Chem. Soc.* 136 (2014) 8564-8567.
- [15] S. Biswas, B. Dutta, K. Mullick, C.-H. Kuo, A. S. Poyraz, S. L. Suib, *ACS Catal.* 5 (2015) 4394-4403.
- [16] B. Dutta, S. Biswas, V. Sharma, N. O. Savage, S. Alpay, S. L. Suib, *Angew. Chem.* 128 (2016) 2211-2215.
- [17] W. Yang, Z. Sua, Z. Xu, W. Yang, Y. Peng, J. Li, *Applied Catalysis B: Environmental* 260 (2020) 118150.

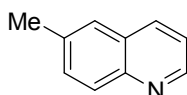
8. Spectrum data of the products

Quinoline (2a)



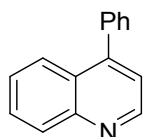
Yellow liquid, isolated yield 98%. ¹H NMR (400 MHz, CDCl₃) δ 8.88 (dt, *J* = 4.2, 2.2 Hz, 1H), 8.09 (d, *J* = 8.5 Hz, 2H), 7.78 – 7.73 (m, 1H), 7.67 (dddd, *J* = 8.5, 6.9, 3.3, 1.4 Hz, 1H), 7.49 (tdd, *J* = 7.0, 3.7, 1.8 Hz, 1H), 7.35 – 7.30 (m, 1H). ¹³C NMR (101 MHz, CDCl₃) δ 150.38, 148.28, 136.00, 129.42, 128.26, 127.76, 126.50, 121.03.

6-methylquinoline (2b)



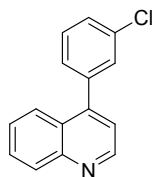
Yellow liquid, isolated yield 98%. ^1H NMR (400 MHz, CDCl_3) δ 8.84 (s, 1H), 8.04 (dd, $J = 20.1, 8.3$ Hz, 2H), 7.54 (d, $J = 12.5$ Hz, 2H), 7.38 – 7.34 (m, 1H), 2.52 (s, 3H). ^{13}C NMR (101 MHz, CDCl_3) δ 149.10, 146.33, 136.61, 135.86, 132.00, 128.44, 126.61, 121.10, 21.57.

4-phenylquinoline (2c)



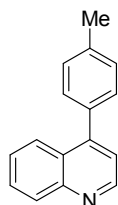
Yellow solid, isolated yield 76%. ^1H NMR (400 MHz, CDCl_3) δ 8.95 (d, $J = 4.4$ Hz, 1H), 8.18 (d, $J = 8.4$ Hz, 1H), 7.93 (d, $J = 8.3$ Hz, 1H), 7.73 (t, $J = 7.1$ Hz, 1H), 7.53 – 7.47 (m, 6H), 7.34 (d, $J = 4.4$ Hz, 1H). ^{13}C NMR (101 MHz, CDCl_3) δ 150.01, 148.69, 138.01, 129.86, 129.57, 129.36, 128.53, 126.65, 125.90, 121.37.

4-(3-chlorophenyl)quinolone (2d)



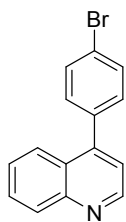
Yellow solid, isolated yield 78%. ^1H NMR (400 MHz, CDCl_3) δ 8.95 (d, $J = 4.4$ Hz, 1H), 8.18 (d, $J = 8.4$ Hz, 1H), 7.86 (d, $J = 8.4$ Hz, 1H), 7.74 (t, $J = 7.6$ Hz, 1H), 7.56 – 7.45 (m, 4H), 7.41 – 7.36 (m, 1H), 7.32 (d, $J = 4.3$ Hz, 1H). ^{13}C NMR (101 MHz, CDCl_3) δ 149.95, 148.63, 146.91, 139.73, 134.57, 129.93, 129.54, 128.59, 127.76, 126.98, 126.40, 125.48, 121.27.

4-(p-tolyl)quinolone (2e)



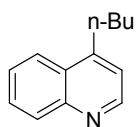
Yellow solid, isolated yield 70%. ^1H NMR (400 MHz, CDCl_3) δ 8.93 (d, $J = 4.4$ Hz, 1H), 8.17 (d, $J = 8.4$ Hz, 1H), 7.96 (d, $J = 8.4$ Hz, 1H), 7.72 (t, $J = 7.6$ Hz, 1H), 7.50 (t, $J = 7.6$ Hz, 1H), 7.41 (d, $J = 7.9$ Hz, 2H), 7.36 – 7.31 (m, 3H), 2.47 (s, 3H). ^{13}C NMR (101 MHz, CDCl_3) δ 150.02, 148.64, 138.41, 135.07, 129.82, 129.33, 126.88, 126.55, 125.98, 121.34, 21.36.

4-(4-bromophenyl)quinolone (2f)



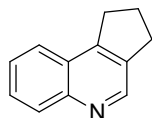
Yellow solid, isolated yield 86%. ^1H NMR (400 MHz, CDCl_3) δ 8.94 (s, 1H), 8.18 (d, $J = 8.3$ Hz, 1H), 7.85 (d, $J = 8.2$ Hz, 1H), 7.73 (t, $J = 7.2$ Hz, 1H), 7.65 (d, $J = 7.9$ Hz, 2H), 7.51 (t, $J = 7.4$ Hz, 1H), 7.37 (d, $J = 7.9$ Hz, 2H), 7.30 (s, 1H). ^{13}C NMR (101 MHz, CDCl_3) δ 149.90, 148.57, 147.25, 136.80, 131.82, 131.13, 129.91, 129.56, 126.92, 126.41, 125.48, 122.87, 121.19.

3,4-dihydroisoquinoline (2g)



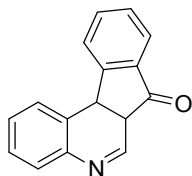
Yellow liquid, isolated yield 82%. ^1H NMR (400 MHz, CDCl_3) δ 8.79 (d, $J = 4.4$ Hz, 1H), 8.11 (d, $J = 8.4$ Hz, 1H), 8.04 (d, $J = 8.4$ Hz, 1H), 7.69 (t, $J = 7.6$ Hz, 1H), 7.55 (t, $J = 7.6$ Hz, 1H), 7.22 (d, $J = 4.4$ Hz, 1H), 3.09 – 3.04 (m, 2H), 1.73 (dd, $J = 15.4, 7.9$ Hz, 2H), 1.46 (dd, $J = 15.0, 7.4$ Hz, 2H), 0.97 (t, $J = 7.3$ Hz, 3H). ^{13}C NMR (101 MHz, CDCl_3) δ 150.17, 148.78, 148.30, 130.18, 128.96, 127.61, 126.19, 123.61, 120.77, 32.20, 31.88, 22.77, 13.93.

2,3-dihydro-1H-cyclopenta[c]quinoline (2h)



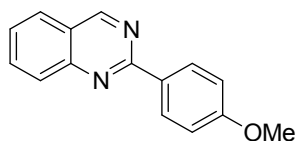
Yellow solid, isolated yield 82%. ^1H NMR (400 MHz, CDCl_3) δ 8.83 (s, 1H), 8.11 (d, $J = 8.4$ Hz, 1H), 7.80 (d, $J = 8.2$ Hz, 1H), 7.65 (t, $J = 7.7$ Hz, 1H), 7.53 (t, $J = 7.5$ Hz, 1H), 3.28 (t, $J = 7.6$ Hz, 2H), 3.14 (t, $J = 7.4$ Hz, 2H), 2.33 – 2.24 (m, 2H). ^{13}C NMR (101 MHz, CDCl_3) δ 149.97, 147.84, 136.72, 129.73, 128.26, 126.37, 126.09, 124.23, 31.35, 30.97, 24.44.

7H-indeno[2,1-c]quinolin-7-one (2i)



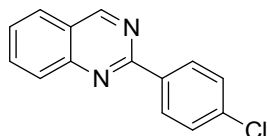
Yellow solid, isolated yield 61%. ^1H NMR (400 MHz, CDCl_3) δ 9.10 (s, 1H), 8.40 (d, $J = 8.4$ Hz, 1H), 8.13 (d, $J = 8.5$ Hz, 1H), 8.04 (d, $J = 7.5$ Hz, 1H), 7.81 (t, $J = 7.4$ Hz, 1H), 7.72 (d, $J = 7.3$ Hz, 1H), 7.65 (t, $J = 7.4$ Hz, 1H), 7.58 (t, $J = 7.3$ Hz, 1H), 7.45 (t, $J = 7.4$ Hz, 1H). ^{13}C NMR (101 MHz, CDCl_3) δ 192.92, 152.58, 151.07, 144.80, 142.47, 134.67, 133.97, 132.11, 131.10, 128.21, 124.88, 124.49, 123.59.

2-(4-methoxyphenyl)quinazoline (4a)



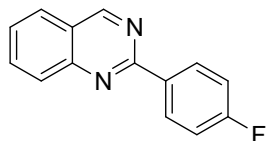
Yellow solid, isolated yield 98%. ^1H NMR (400 MHz, CDCl_3) δ 9.40 (s, 1H), 8.58 (d, $J = 8.6$ Hz, 2H), 8.03 (d, $J = 8.4$ Hz, 1H), 7.87 (d, $J = 7.6$ Hz, 2H), 7.55 (t, $J = 7.5$ Hz, 1H), 7.05 (d, $J = 8.6$ Hz, 2H), 3.89 (s, 3H). ^{13}C NMR (101 MHz, CDCl_3) δ 161.84, 160.86, 160.37, 159.73, 150.84, 133.98, 131.75, 130.75, 130.21, 128.41, 127.11, 126.76, 123.32, 113.98, 55.38.

2-(4-chlorophenyl)quinazoline (4b)



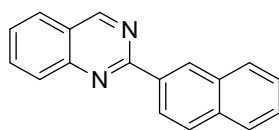
Yellow solid, isolated yield 92%, ^1H NMR (400 MHz, CDCl_3) δ 9.45 (s, 1H), 8.58 (d, $J = 7.2$ Hz, 2H), 8.08 (d, $J = 7.7$ Hz, 1H), 7.93 (d, $J = 7.1$ Hz, 2H), 7.63 (s, 1H), 7.51 (d, $J = 7.5$ Hz, 2H). ^{13}C NMR (101 MHz, CDCl_3) δ 160.51, 160.02, 150.67, 136.83, 136.52, 134.24, 129.90, 128.82, 128.60, 127.45, 127.14, 123.61.

2-(4-fluorophenyl)quinazoline (4c)



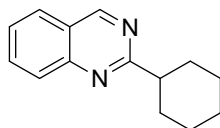
Yellow solid, isolated yield 71%. ^1H NMR (400 MHz, CDCl_3) δ 9.43 (s, 1H), 8.62 (dd, $J = 8.8$, 5.7 Hz, 2H), 8.07 – 8.03 (m, 1H), 7.89 (t, $J = 7.6$ Hz, 2H), 7.60 (t, $J = 7.5$ Hz, 1H), 7.20 (t, $J = 8.7$ Hz, 2H). ^{13}C NMR (101 MHz, CDCl_3) δ 165.92, 163.43, 160.50, 150.71, 134.19, 130.67, 128.54, 127.20, 123.48, 115.65, 115.44.

2-(naphthalen-2-yl)quinazoline (4d)



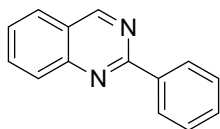
Yellow solid, isolated yield 88%. ^1H NMR (400 MHz, CDCl_3) δ 9.49 (s, 1H), 9.16 (s, 1H), 8.74 (d, $J = 8.6$ Hz, 1H), 8.13 (d, $J = 8.7$ Hz, 1H), 8.07 – 8.03 (m, 1H), 8.00 (d, $J = 8.7$ Hz, 1H), 7.90 (dd, $J = 5.9$, 2.9 Hz, 3H), 7.59 (t, $J = 7.5$ Hz, 1H), 7.56 – 7.52 (m, 2H). ^{13}C NMR (101 MHz, CDCl_3) δ 160.99, 160.51, 150.82, 135.39, 134.70, 134.17, 133.43, 129.30, 128.98, 128.64, 128.30, 127.74, 127.57 – 127.02, 126.25, 125.44, 123.63.

2-cyclohexylquinazoline (4e)



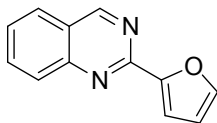
Yellow oily liquid. Isolated yield 93%. ^1H NMR (400 MHz, CDCl_3) δ 9.33 (s, 1H), 7.96 (d, J = 8.4 Hz, 1H), 7.85 (d, J = 7.6 Hz, 2H), 7.55 (t, J = 7.3 Hz, 1H), 3.04 (t, J = 11.6 Hz, 1H), 2.07 (d, J = 12.2 Hz, 2H), 1.88 (d, J = 12.0 Hz, 2H), 1.76 (d, J = 12.1 Hz, 3H), 1.45 (d, J = 12.7 Hz, 1H), 1.34 (d, J = 14.1 Hz, 1H), 1.25 (d, J = 11.7 Hz, 1H). ^{13}C NMR (101 MHz, CDCl_3) δ 170.89, 160.32, 133.80, 127.01, 126.79, 123.27, 47.93, 31.95, 26.32, 26.04.

2-phenylquinazoline (4f)



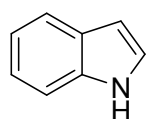
Yellow solid. Isolated yield 65%. ^1H NMR (400 MHz, CDCl_3) δ 9.46 (d, J = 0.7 Hz, 1H), 8.66 – 8.60 (m, 2H), 8.11 – 8.07 (m, 1H), 7.93 – 7.87 (m, 2H), 7.62 – 7.51 (m, 4H). ^{13}C NMR (101 MHz, CDCl_3) δ 160.07, 159.44, 149.78, 137.06, 133.04, 129.57, 127.61, 126.14, 122.60.

2-(furan-2-yl)quinazoline (4g)



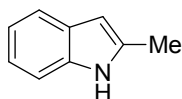
Yellow solid, isolated yield 38%, ^1H NMR (400 MHz, CDCl_3) δ 9.34 (s, 1H), 8.06 (d, J = 8.8 Hz, 1H), 7.86 (t, J = 7.8 Hz, 2H), 7.67 (d, J = 0.7 Hz, 1H), 7.55 (t, J = 7.5 Hz, 1H), 7.44 (d, J = 2.9 Hz, 1H), 6.59 (dd, J = 2.1, 1.2 Hz, 1H). ^{13}C NMR (101 MHz, CDCl_3) δ 160.69, 154.10, 152.53, 150.42, 145.31, 134.46, 128.94, 128.37, 127.23, 123.36, 114.08, 112.30.

1H-indole (4h)



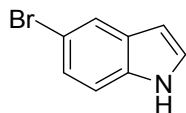
White solid, isolated yield 91%. ^1H NMR (400 MHz, CDCl_3) δ 8.00 (s, 1H), 7.58 (d, J = 7.7 Hz, 1H), 7.29 (d, J = 8.0 Hz, 1H), 7.08 (tt, J = 14.9, 7.3 Hz, 3H), 6.48 (s, 1H). ^{13}C NMR (101 MHz, CDCl_3) δ 135.82, 127.89, 124.17, 122.01, 120.76, 119.84, 111.06, 102.63.

2-methyl-1H-indole (4i)



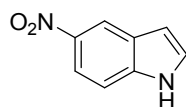
White solid, isolated yield 69%. ^1H NMR (400 MHz, CDCl_3) δ 7.80 (s, 1H), 7.52 (d, $J = 7.5$ Hz, 1H), 7.27 (d, $J = 7.8$ Hz, 1H), 7.16 – 7.03 (m, 2H), 6.22 (s, 1H), 2.43 (s, 3H). ^{13}C NMR (101 MHz, CDCl_3) δ 136.08, 135.02, 129.10, 120.95, 119.63, 110.19, 100.40, 13.68.

5-bromo-1H-indole (4j)



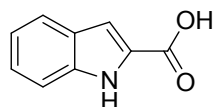
Yellow solid, isolated yield 79%. ^1H NMR (400 MHz, CDCl_3) δ 8.19 (s, 1H), 7.80 (s, 1H), 7.32 – 7.26 (m, 2H), 7.22 (t, $J = 2.6$ Hz, 1H), 6.52 (s, 1H). ^{13}C NMR (101 MHz, CDCl_3) δ 134.38, 129.61, 125.32, 124.81, 123.18, 112.99, 112.39, 102.28.

5-nitro-1H-indole (4k)



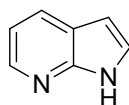
Yellow solid, isolated yield 78%. ^1H NMR (400 MHz, DMSO) δ 11.84 (s, 1H), 8.58 (s, 1H), 8.00 (dd, $J = 8.9, 1.9$ Hz, 1H), 7.63 (s, 1H), 7.57 (d, $J = 9.0$ Hz, 1H), 6.74 (s, 1H). ^{13}C NMR (101 MHz, DMSO) δ 141.09, 139.52, 129.73, 127.43, 117.70, 116.82, 112.25, 104.34.

1H-indole-2-carboxylic acid (4l)



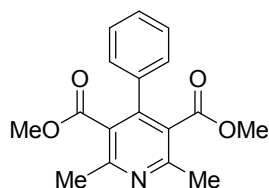
White solid, isolated yield 93%. ^1H NMR (400 MHz, CDCl_3) δ 8.20 (s, 1H), 7.72 (d, $J = 7.7$ Hz, 1H), 7.46 (d, $J = 7.9$ Hz, 1H), 7.28 (d, $J = 18.1$ Hz, 2H), 7.18 (t, $J = 7.3$ Hz, 1H), 6.62 (s, 1H). ^{13}C NMR (101 MHz, CDCl_3) δ 127.87, 124.09, 121.98, 120.73, 119.81, 110.99, 102.65.

1H-pyrrolo[2,3-b]pyridine (4m)



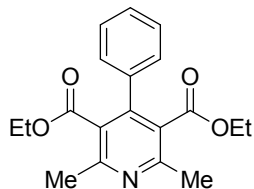
White solid, isolated yield 95%. ^1H NMR (400 MHz, CDCl_3) δ 11.48 (s, 1H), 8.34 (s, 1H), 7.99 (d, $J = 7.6$ Hz, 1H), 7.40 (s, 1H), 7.11 (d, $J = 4.6$ Hz, 1H), 6.52 (s, 1H). ^{13}C NMR (101 MHz, CDCl_3) δ 148.67, 142.10, 129.20, 125.35, 120.68, 115.74, 100.62.

Dimethyl 2,6-dimethyl-4-phenylpyridine-3,5-dicarboxylate (4n)



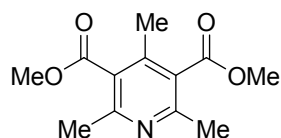
Yellow solid. Isolated yield 99%. ^1H NMR (400 MHz, CDCl_3) δ 7.40 (s, 3H), 7.27 (dd, $J = 4.2$, 3.0 Hz, 2H), 3.55 (d, $J = 0.6$ Hz, 6H), 2.63 (d, $J = 0.5$ Hz, 6H). ^{13}C NMR (101 MHz, CDCl_3) δ 168.36 (s), 155.55 (s), 146.27 (s), 136.40 (s), 128.57 (d, $J = 7.8$ Hz), 128.21, 127.74, 126.80, 52.16, 22.86.

Diethyl 2,6-dimethyl-4-phenylpyridine-3,5-dicarboxylate (4o)



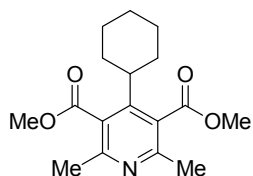
Yellow solid. Isolated yield 92%. ^1H NMR (400 MHz, CDCl_3) δ 7.36 (s, 2H), 7.28 – 7.22 (m, 1H), 4.04 – 3.96 (m, 2H), 2.60 (s, 3H), 0.89 (dd, $J = 10.2$, 4.1 Hz, 3H). ^{13}C NMR (101 MHz, CDCl_3) δ 167.86, 155.40, 146.11, 136.57, 128.40, 128.07, 126.91, 61.32, 22.89, 13.53.

Dimethyl 2,4,6-trimethylpyridine-3,5-dicarboxylate (4p)



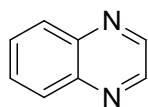
Yellow solid. Isolated yield 92%. ^1H NMR (400 MHz, CDCl_3) δ 3.90 (s, 6H), 2.48 (s, 6H), 2.22 (s, 3H). ^{13}C NMR (101 MHz, CDCl_3) δ 168.84, 155.22, 142.36, 127.29, 52.42, 23.02, 17.12.

Dimethyl 4-cyclohexyl-2,6-dimethylpyridine-3,5-dicarboxylate (4q)



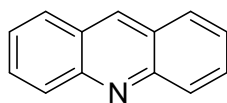
White solid. Isolated yield 79%. ^1H NMR (400 MHz, CDCl_3) δ 8.67 (s, 1H), 3.90 (s, 7H), 2.82 (s, 7H). ^{13}C NMR (101 MHz, CDCl_3) δ 166.19, 162.62, 141.04, 122.59, 52.29, 24.93.

Quinoxaline (4r)



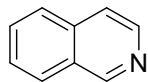
Yellow liquid, isolated yield 98%. ^1H NMR (400 MHz, CDCl_3) δ 8.85 (s, 1H), 8.11 (d, $J = 3.5$ Hz, 1H), 7.77 (d, $J = 3.5$ Hz, 1H). ^{13}C NMR (101 MHz, CDCl_3) δ 144.88, 142.88, 130.19, 129.36.

Acridine (4s)



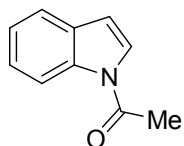
White solid, isolated yield 99%. ^1H NMR (400 MHz, CDCl_3) δ 8.72 (s, 1H), 8.25 (d, $J = 8.7$ Hz, 2H), 7.96 (d, $J = 8.2$ Hz, 2H), 7.77 (t, $J = 7.4$ Hz, 2H), 7.51 (t, $J = 7.2$ Hz, 2H). ^{13}C NMR (101 MHz, CDCl_3) δ 148.93, 136.19, 130.38, 129.21, 128.19, 126.57, 125.69.

Isoquinoline (4t)

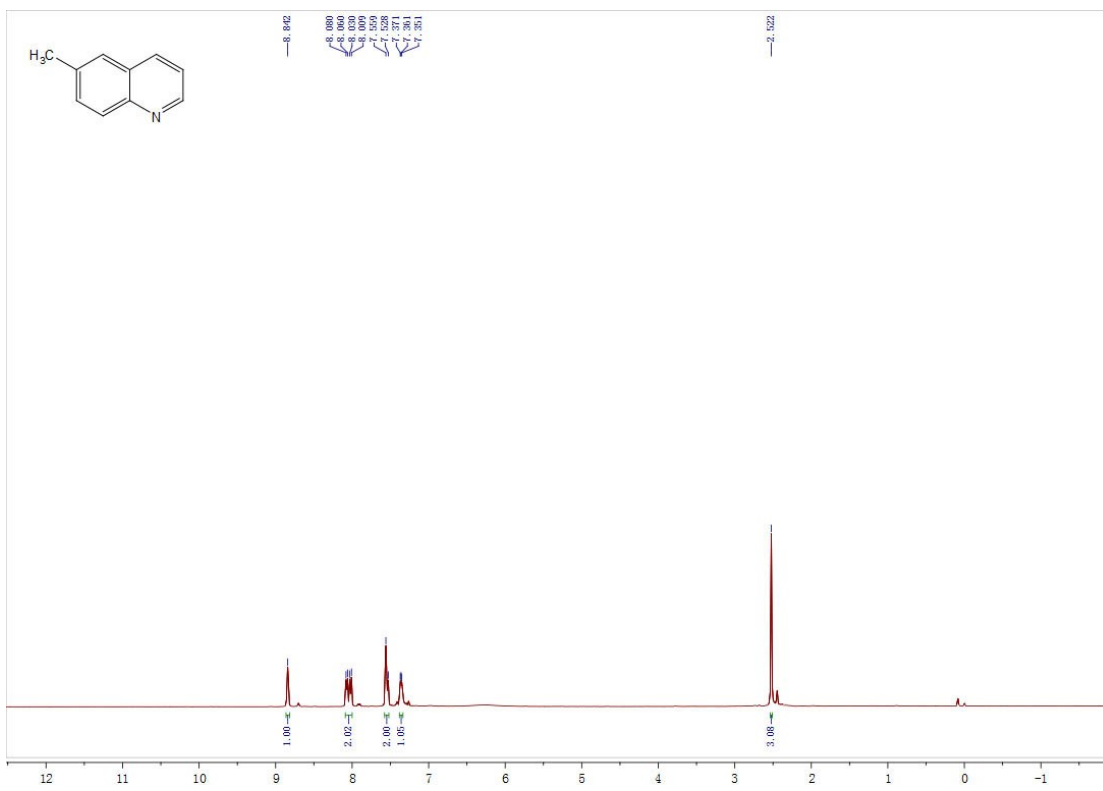


Colorless oil liquid. Isolated yield 58%. ^1H NMR (400 MHz, CDCl_3) δ 8.88 (dt, $J = 4.2, 2.2$ Hz, 1H), 8.09 (d, $J = 8.5$ Hz, 2H), 7.78 – 7.73 (m, 1H), 7.67 (dddd, $J = 8.5, 6.9, 3.3, 1.4$ Hz, 1H), 7.49 (tdd, $J = 7.0, 3.7, 1.8$ Hz, 1H), 7.35 – 7.30 (m, 1H). ^{13}C NMR (101 MHz, CDCl_3) δ 150.38, 148.28, 136.00, 129.42, 128.26, 127.76, 126.50, 121.03.

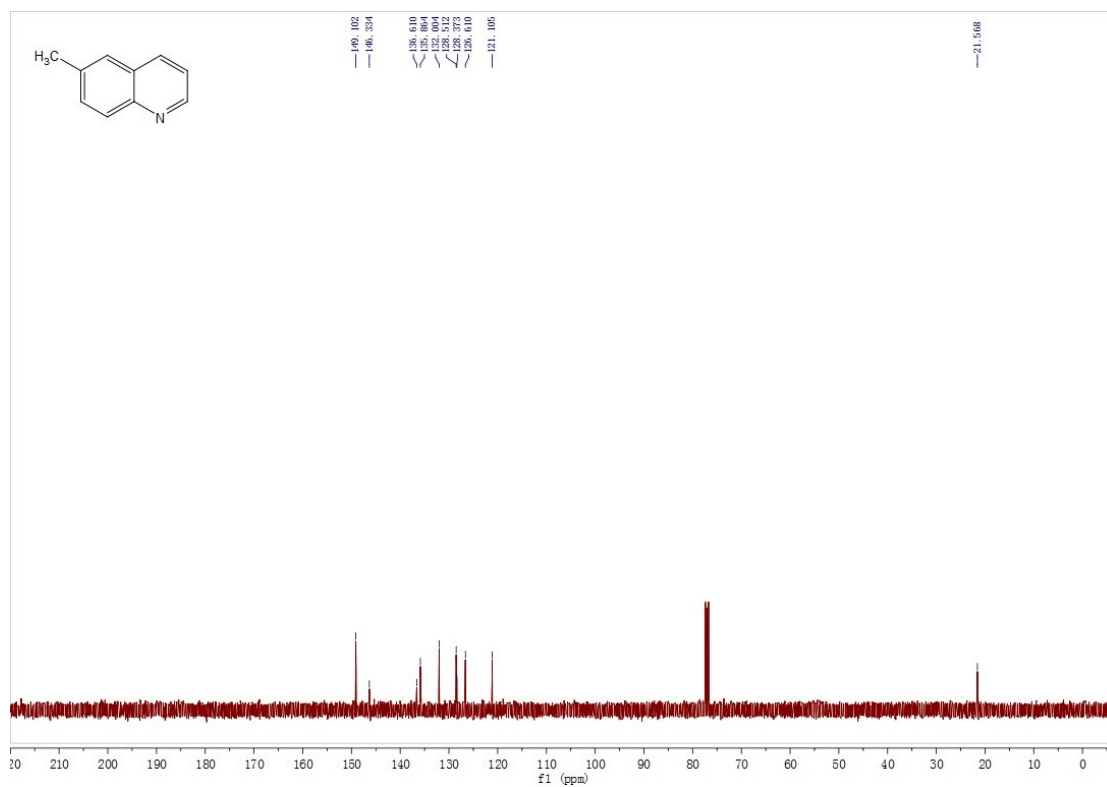
1-(1H-indol-1-yl)ethanone (7b)



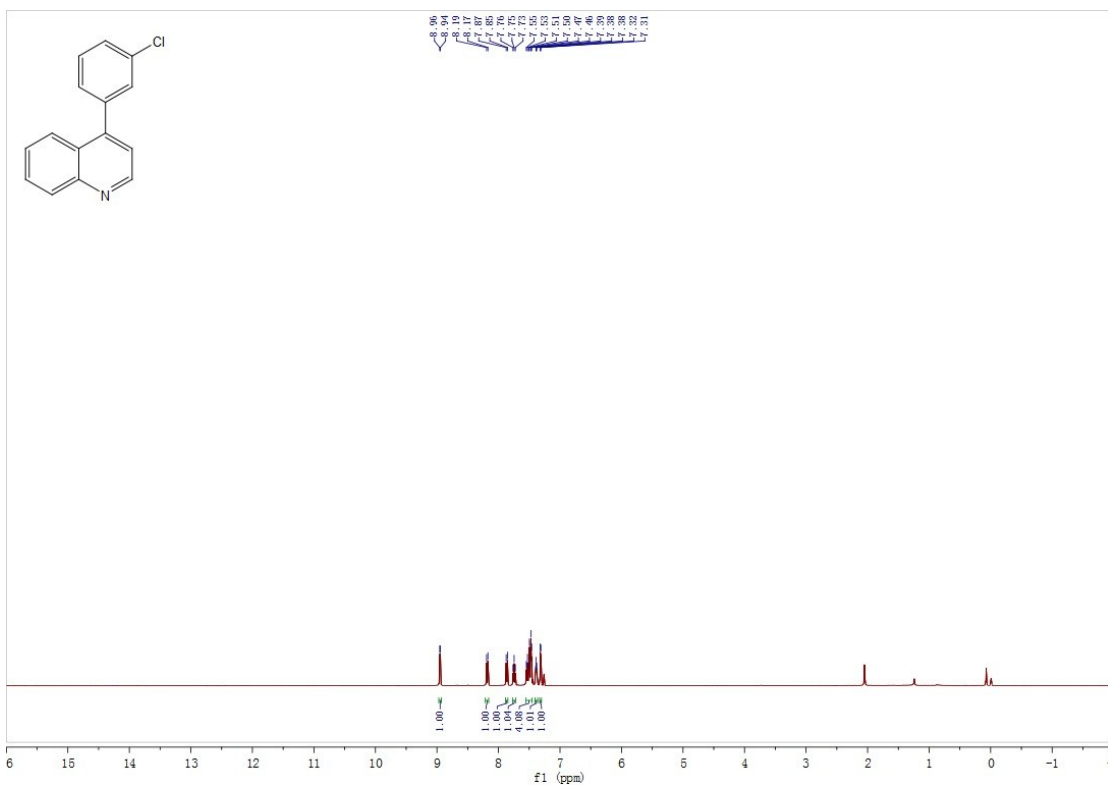
^1H NMR (400 MHz, CDCl_3) δ 8.45 (d, $J = 8.0$ Hz, 1H), 7.57 (d, $J = 7.7$ Hz, 1H), 7.43 (s, 1H), 7.36 (t, $J = 7.7$ Hz, 1H), 7.30 – 7.25 (m, 1H), 6.65 (d, $J = 3.0$ Hz, 1H), 2.65 (s, 3H). ^{13}C NMR (101 MHz, CDCl_3) δ 168.56, 135.58, 130.44, 125.17, 125.11, 123.64, 120.82, 116.53, 109.15, 23.92.



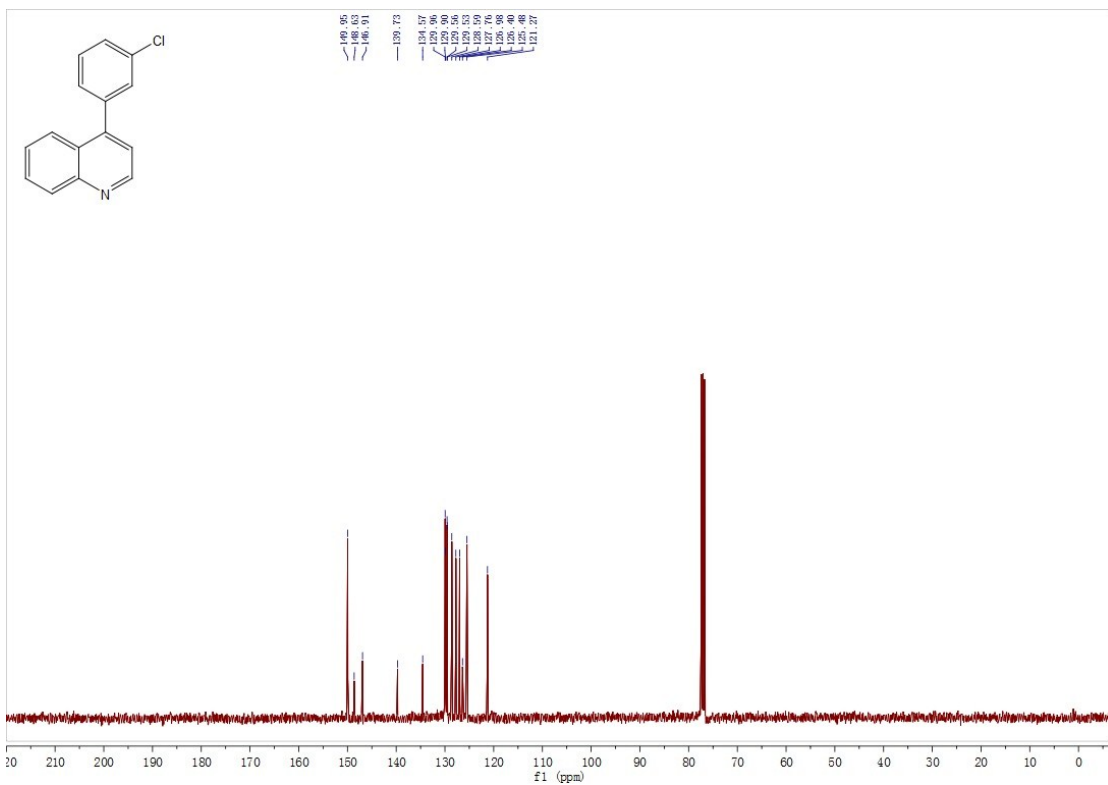
¹H NMR of **2b**



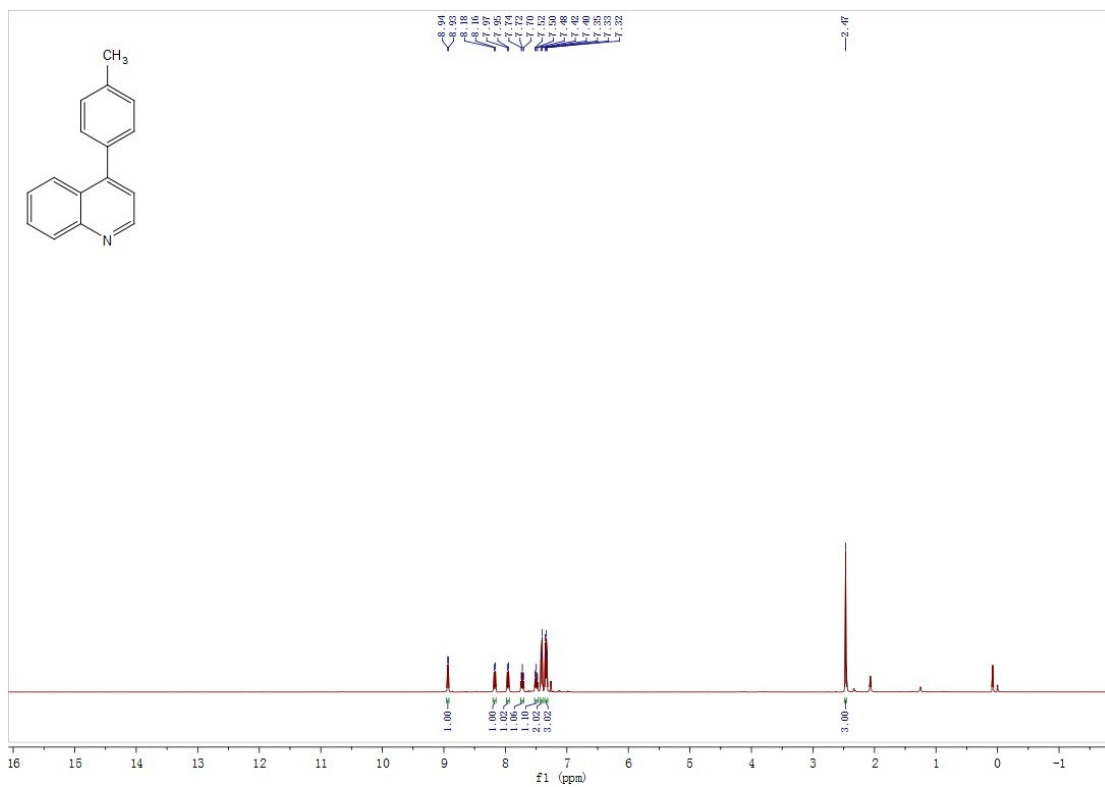
¹³C NMR of **2b**



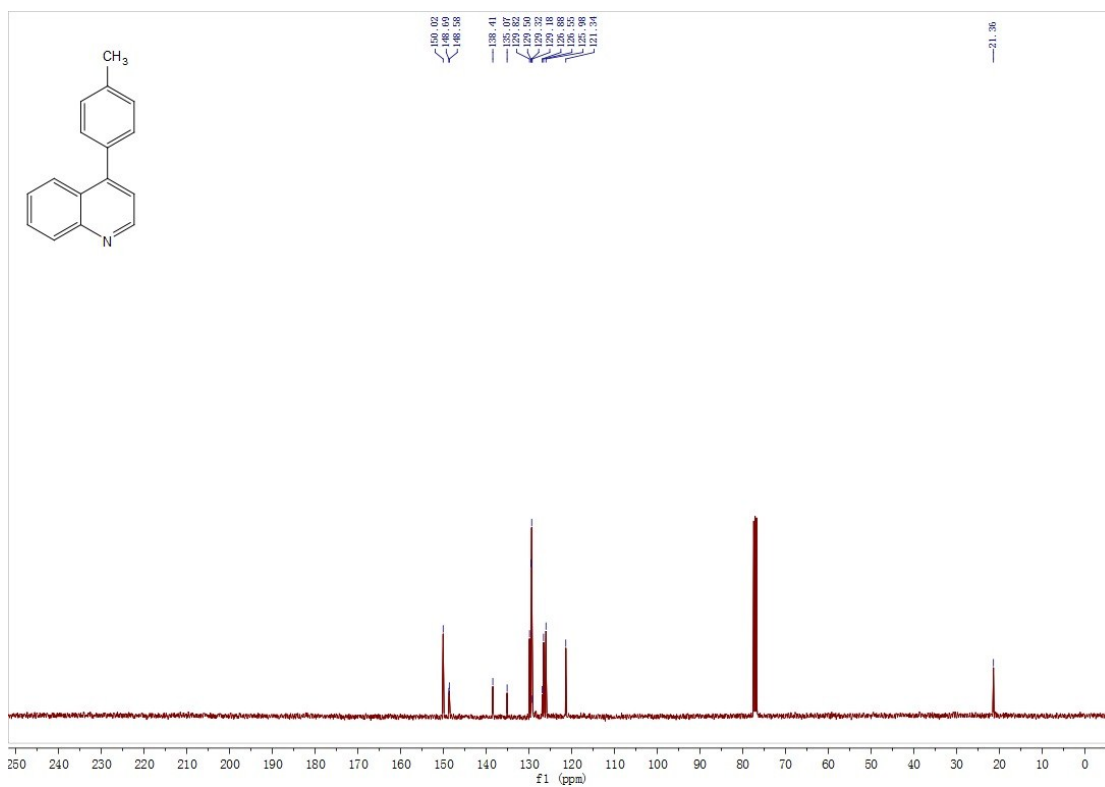
¹H NMR of 2d



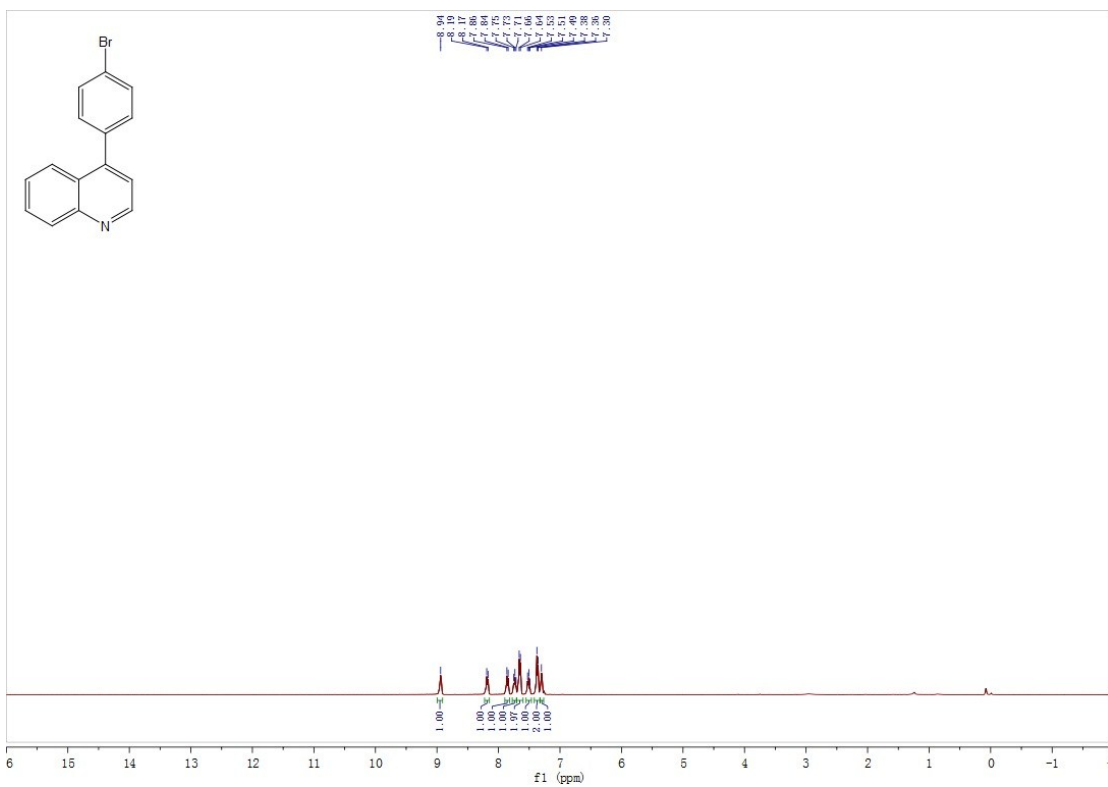
¹³C NMR of 2d



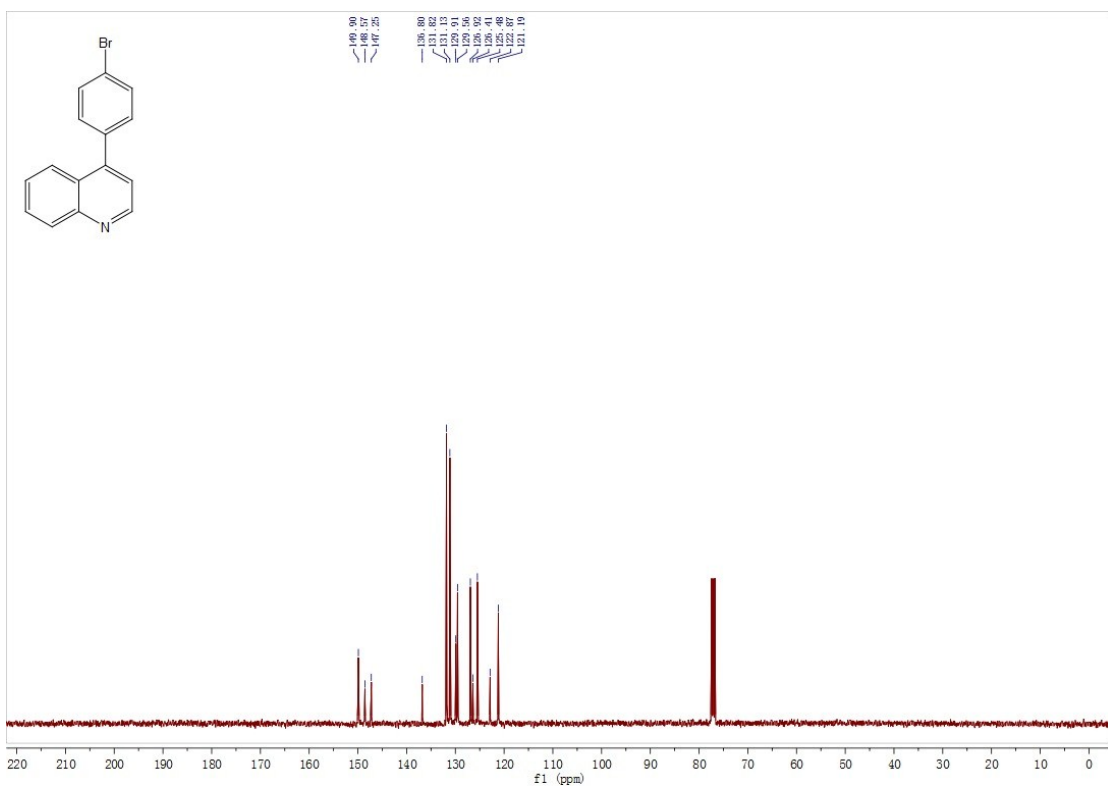
¹H NMR of 2e



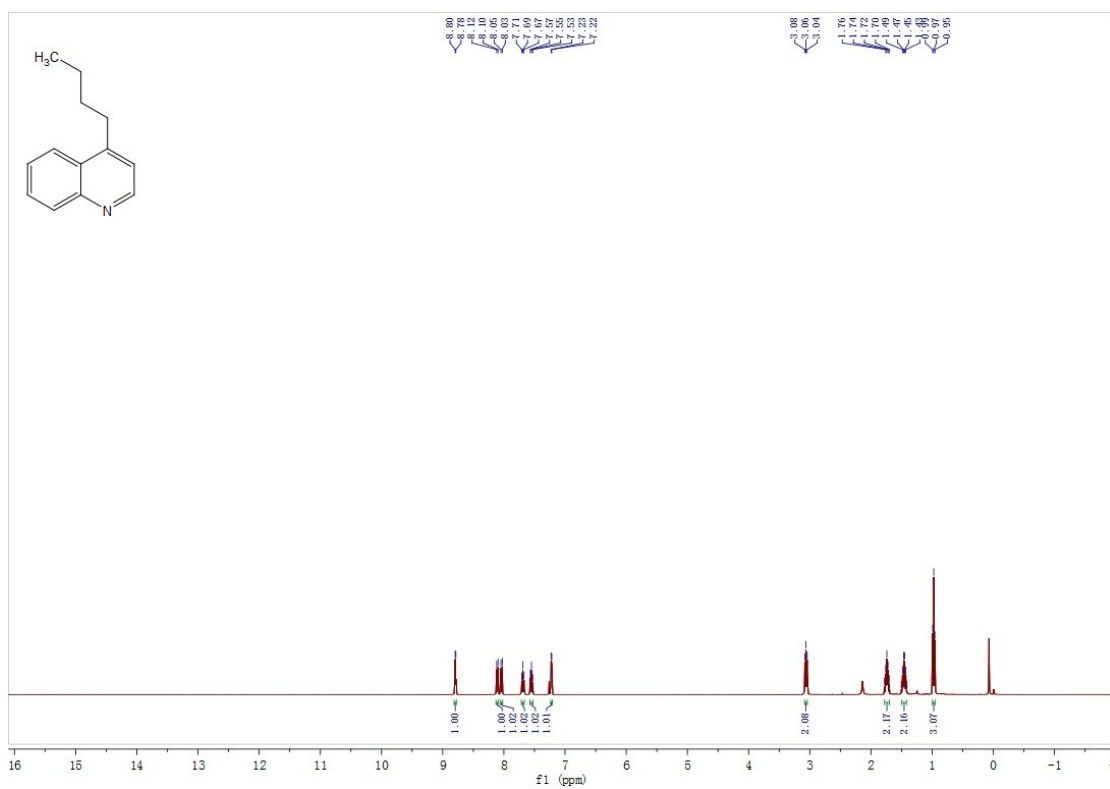
¹³C NMR of 2e



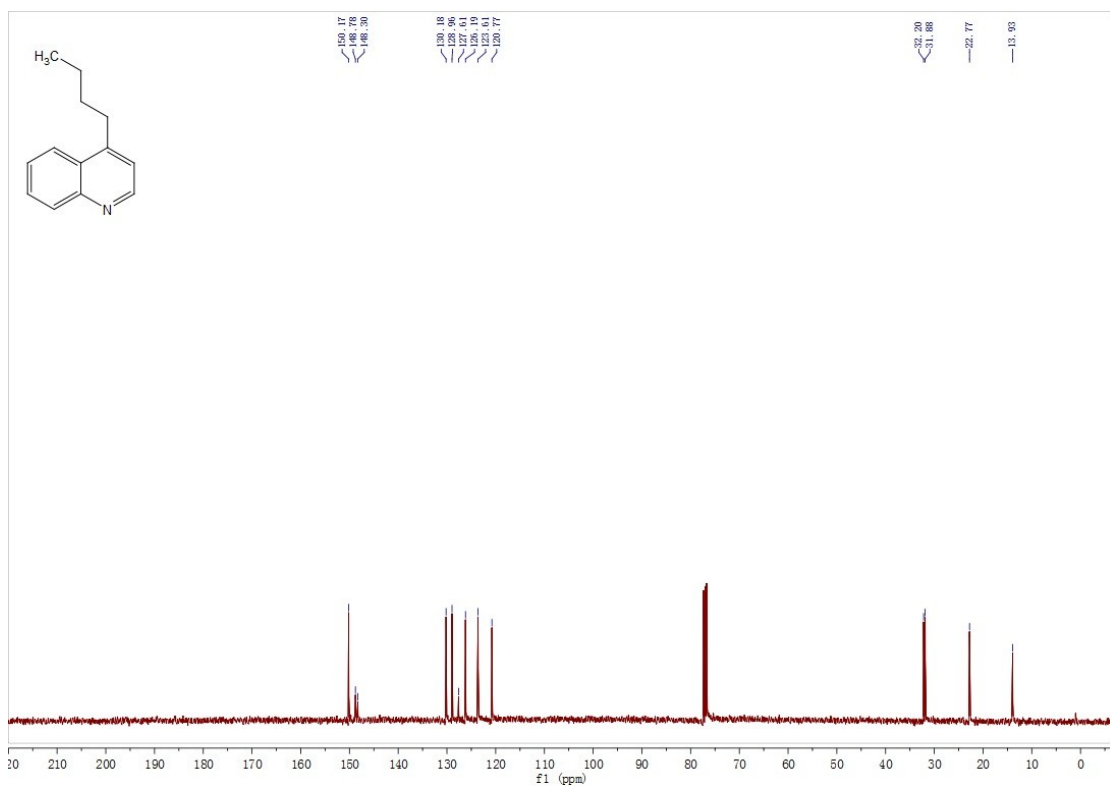
¹H NMR of **2f**



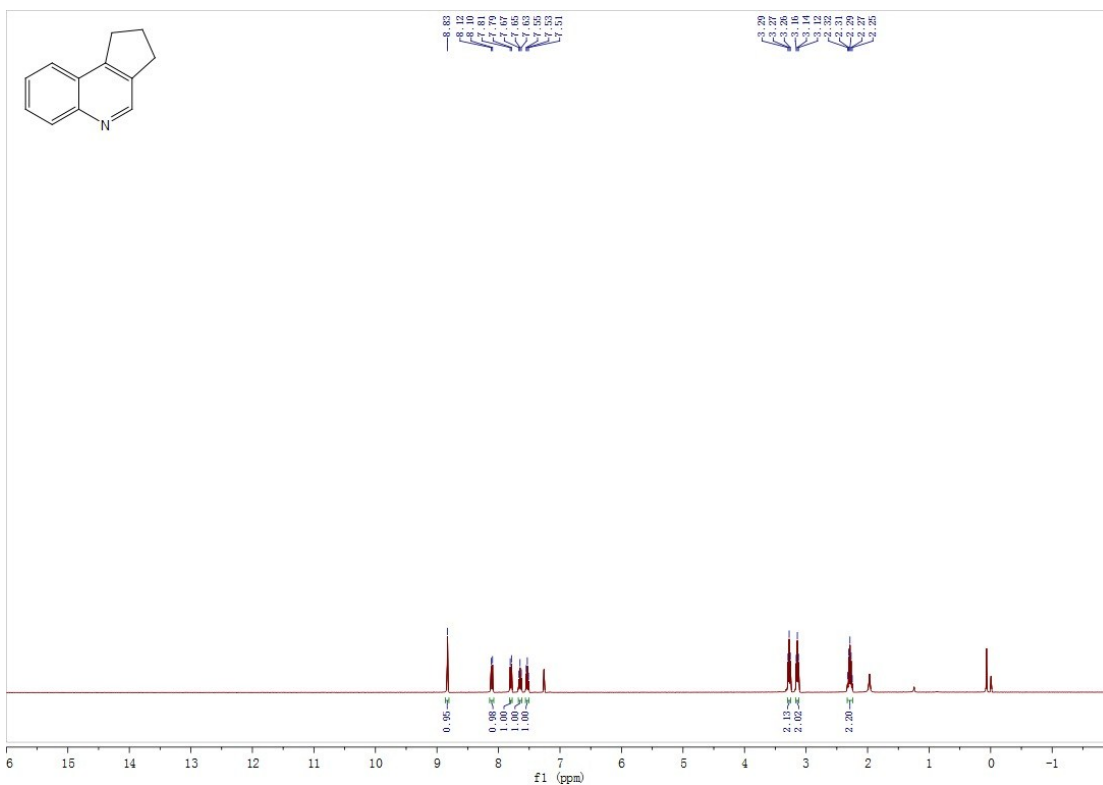
¹³C NMR of **2f**



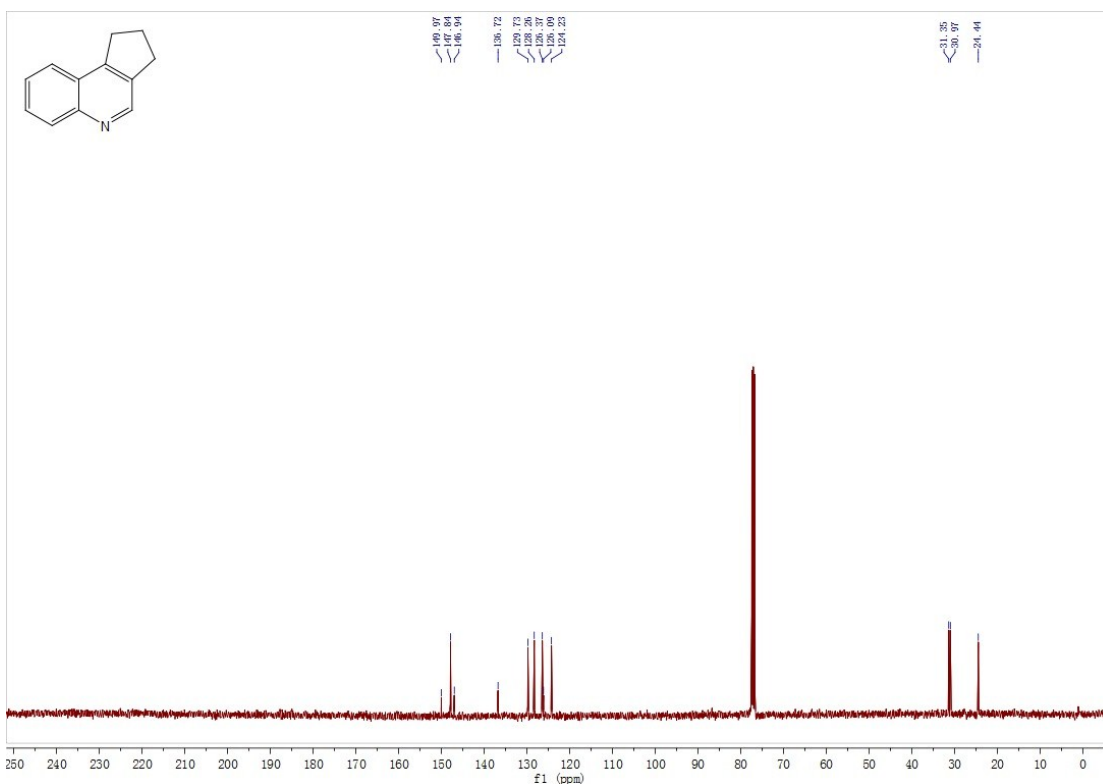
¹H NMR of 2g



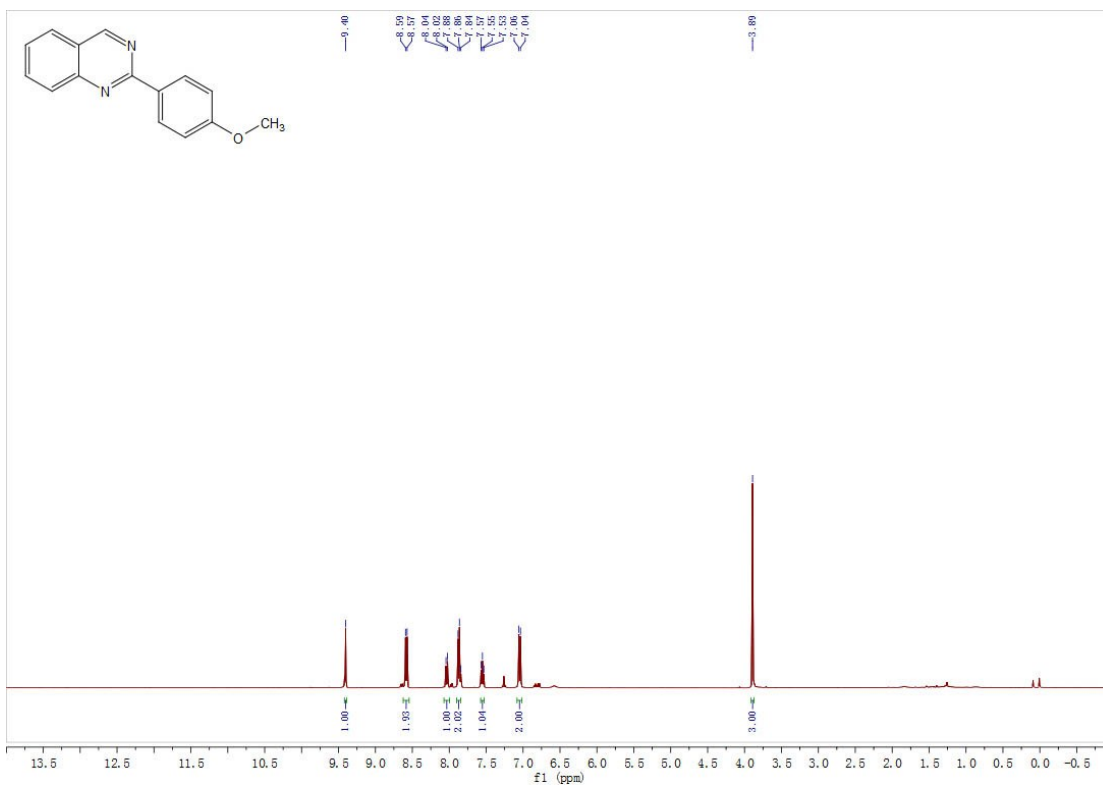
¹³C NMR of 2g



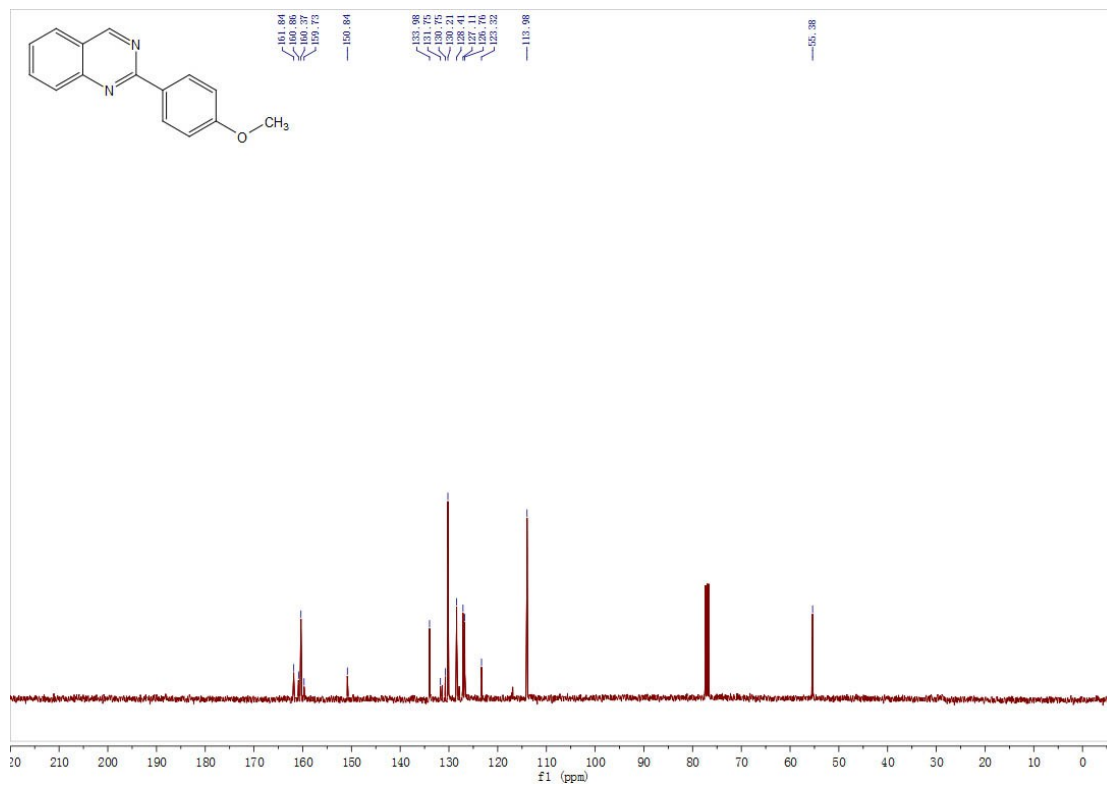
¹H NMR of 2h



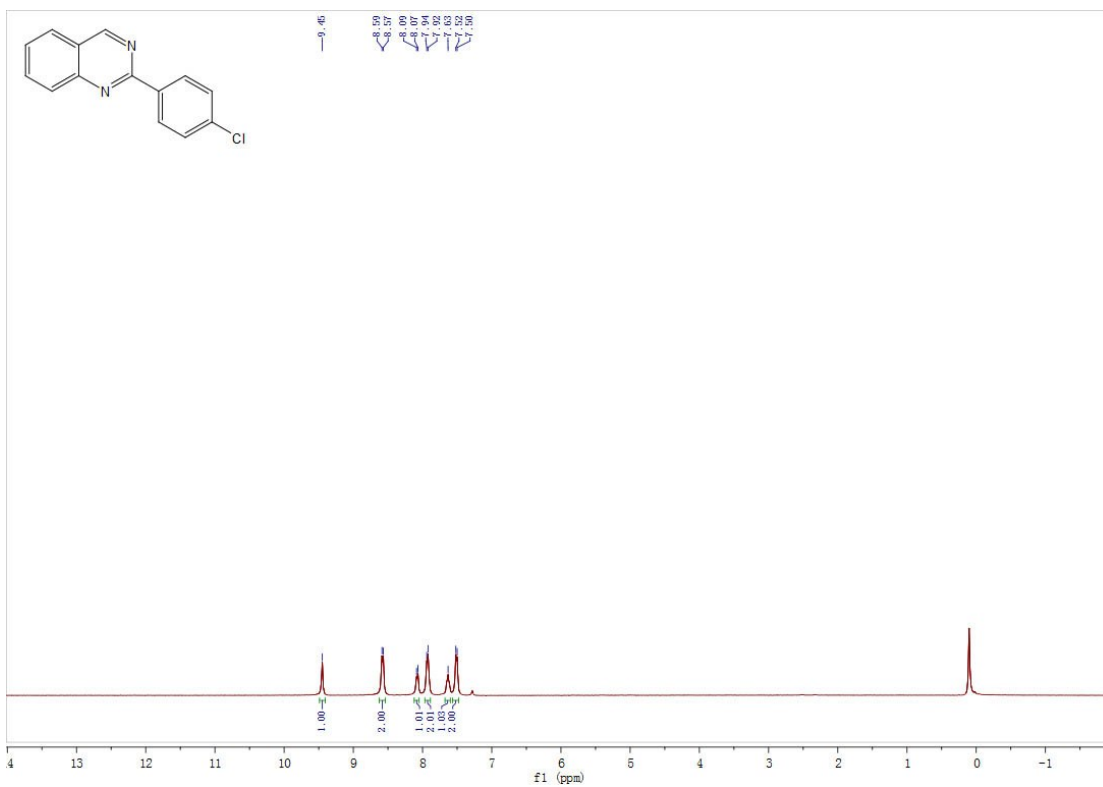
¹³C NMR of 2h



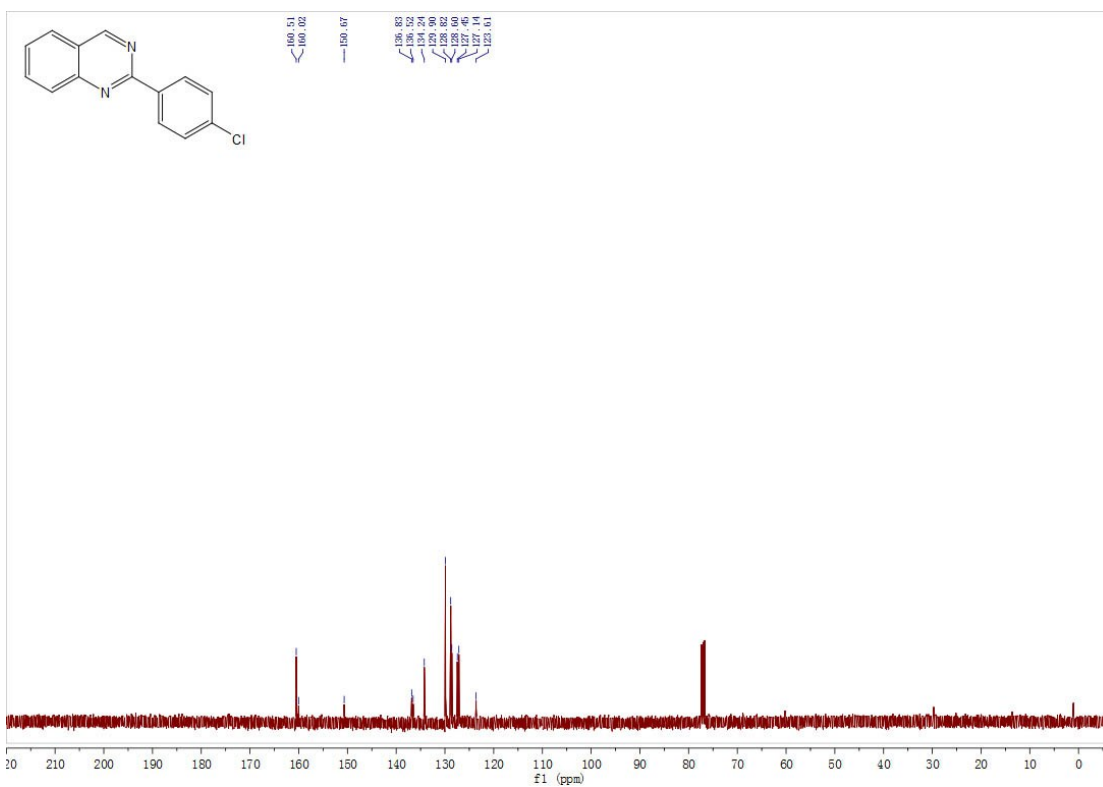
¹H NMR of 4a



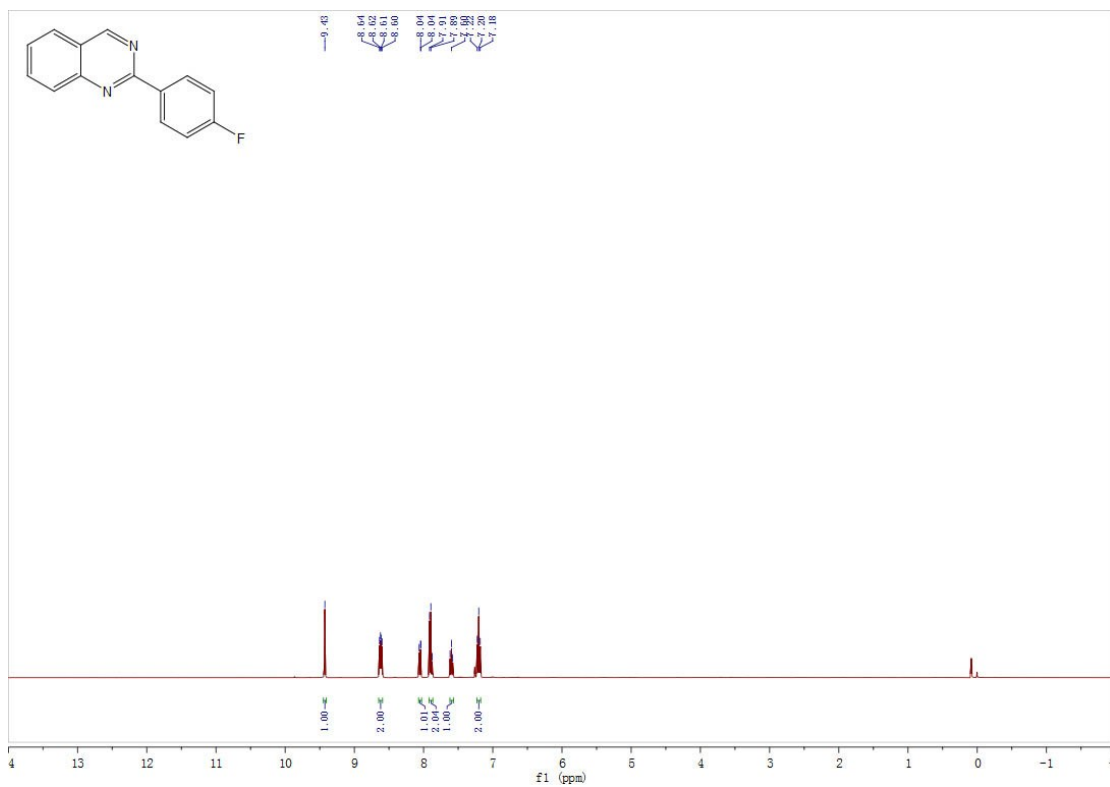
¹³C NMR of 4a



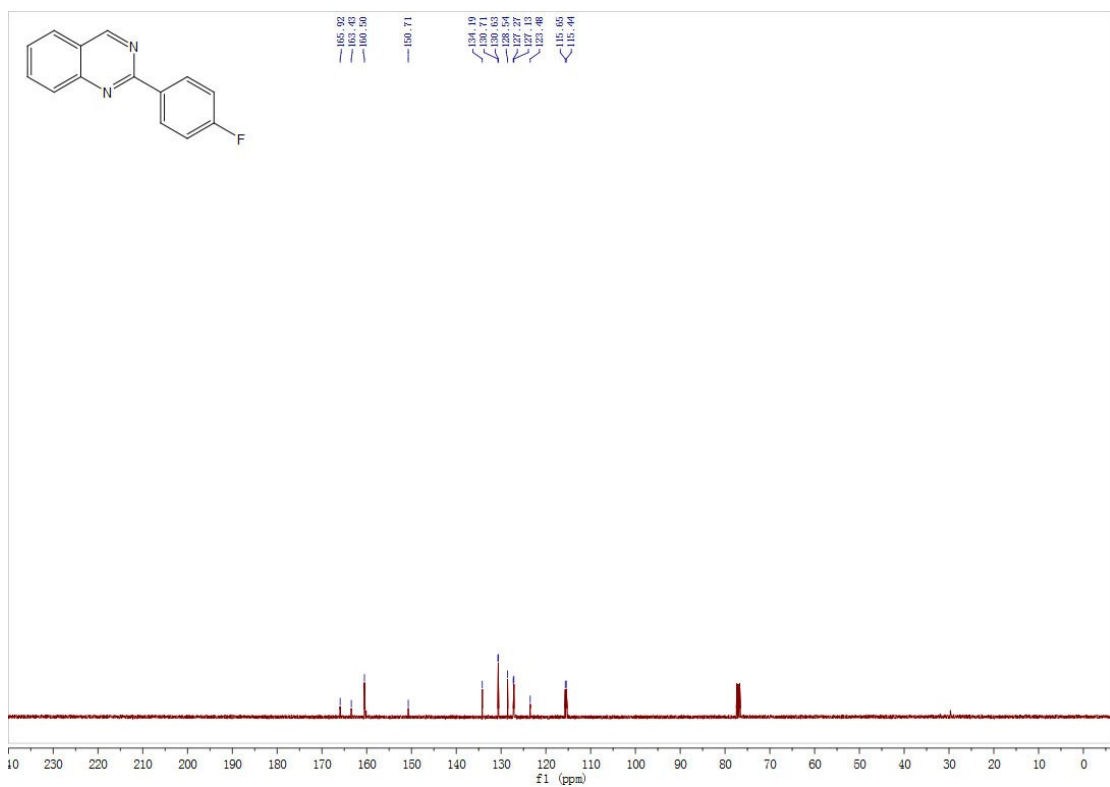
¹H NMR of 4b



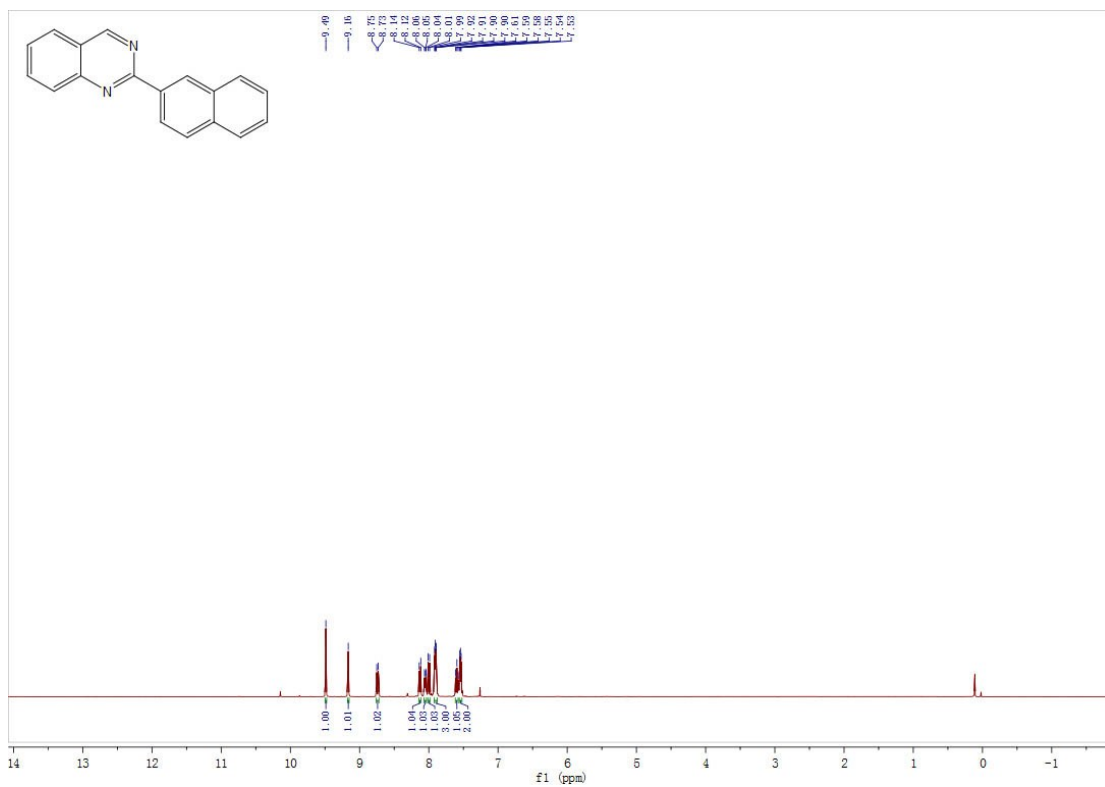
¹³C NMR of 4b



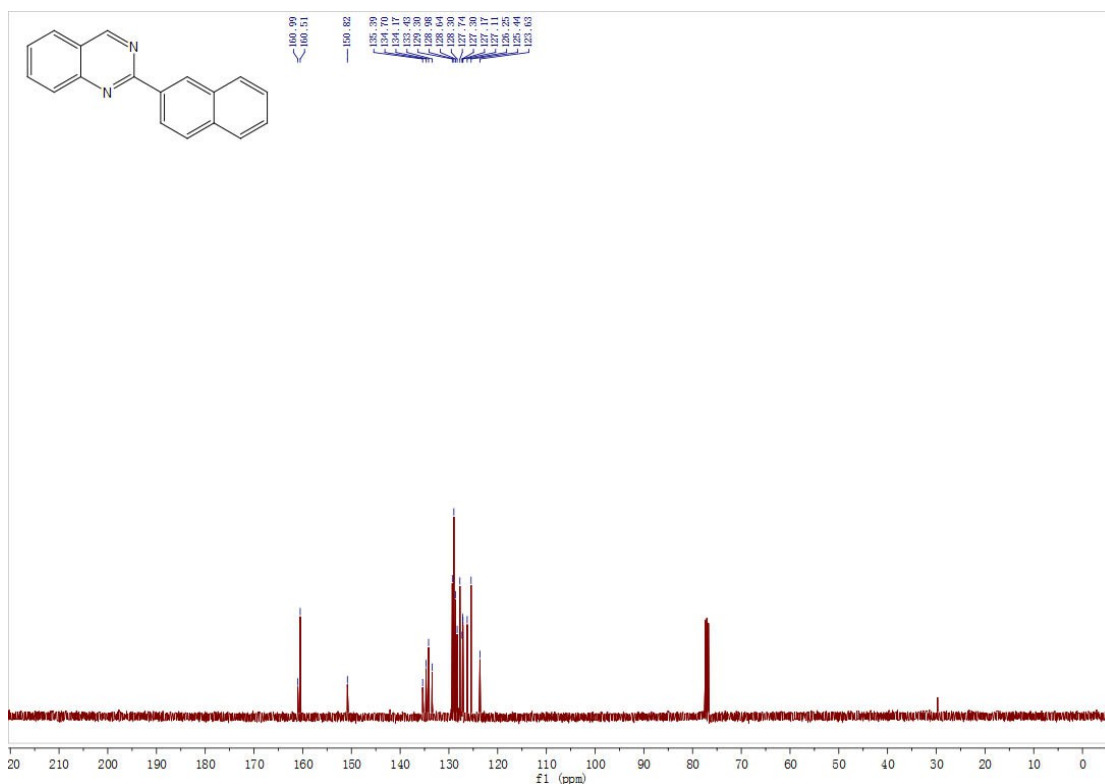
¹H NMR of 4c



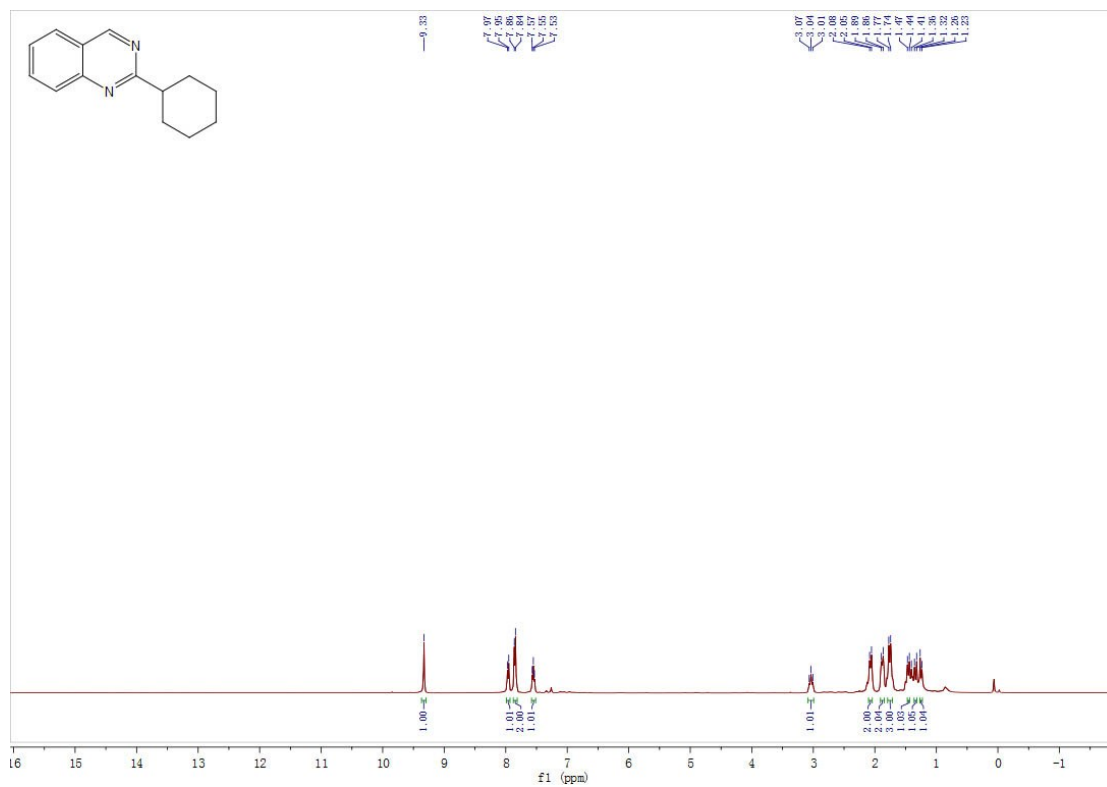
¹³C NMR of 4c



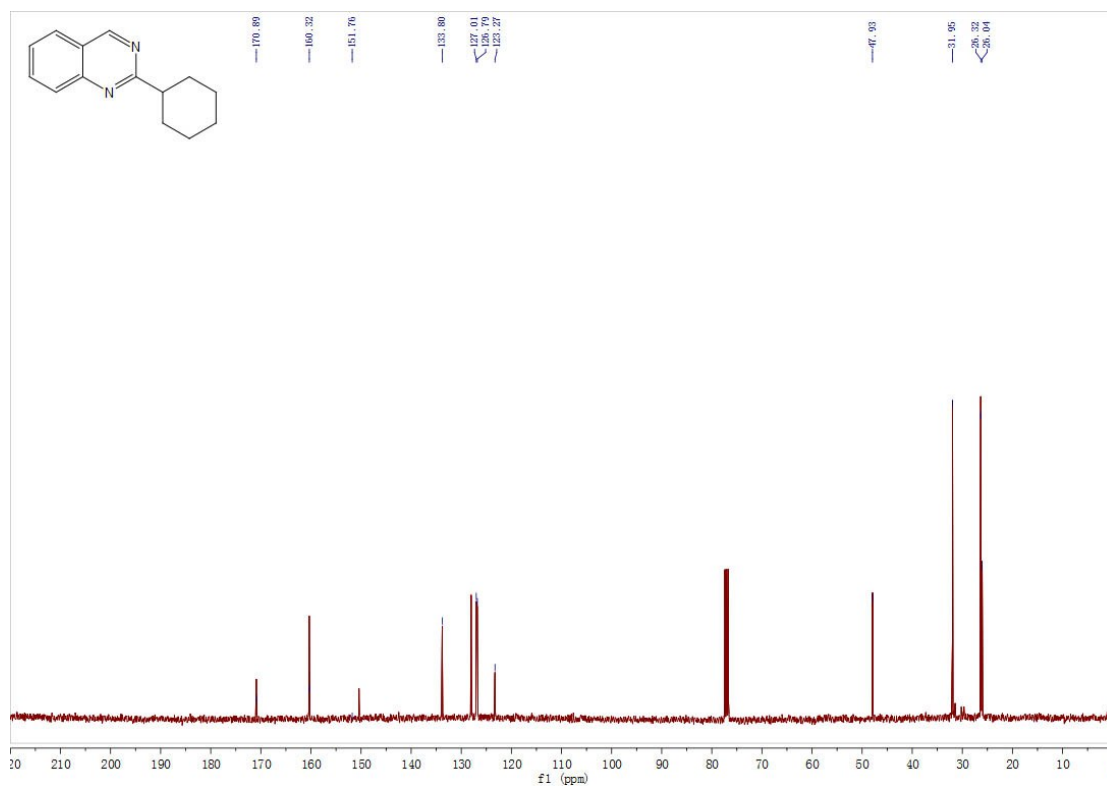
¹H NMR of 4d



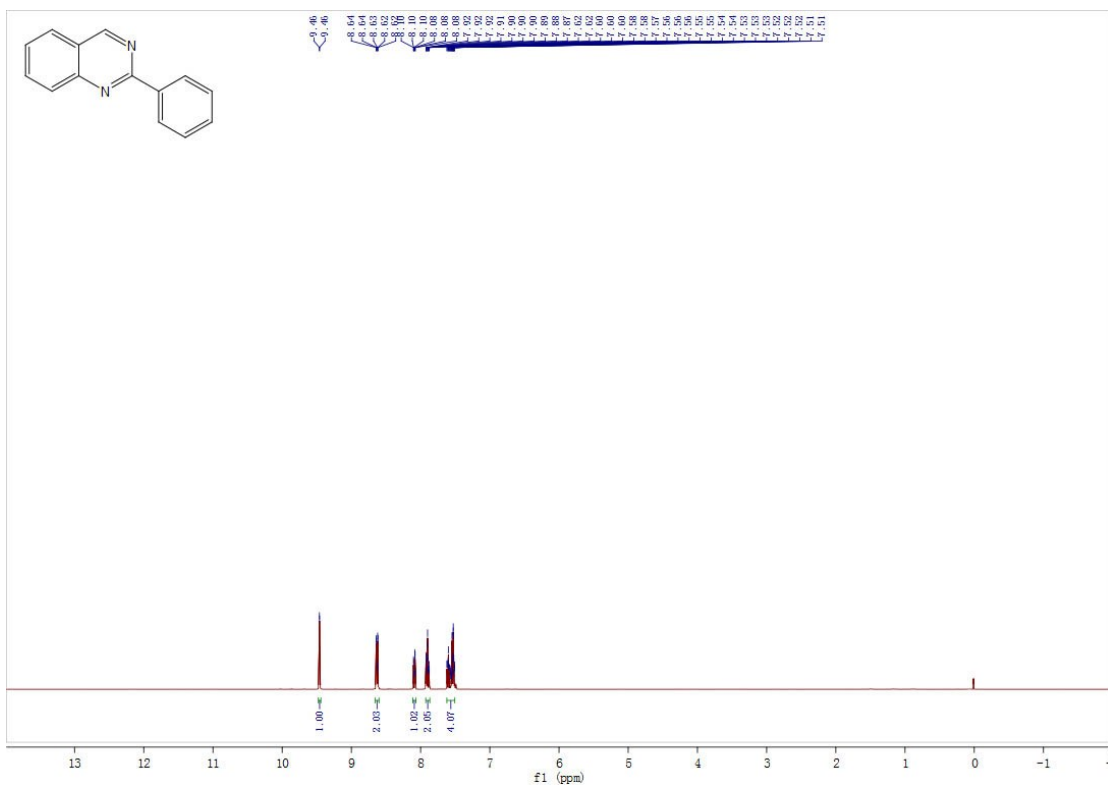
¹³C NMR of 4d



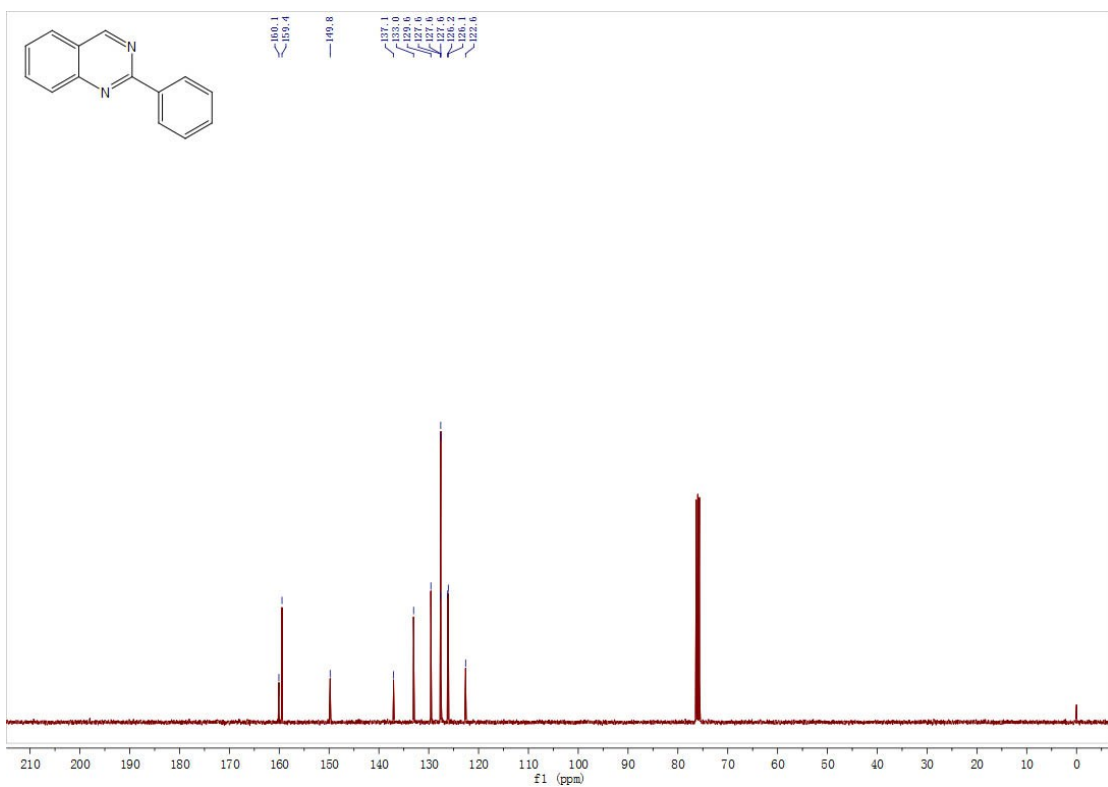
¹H NMR of 4e



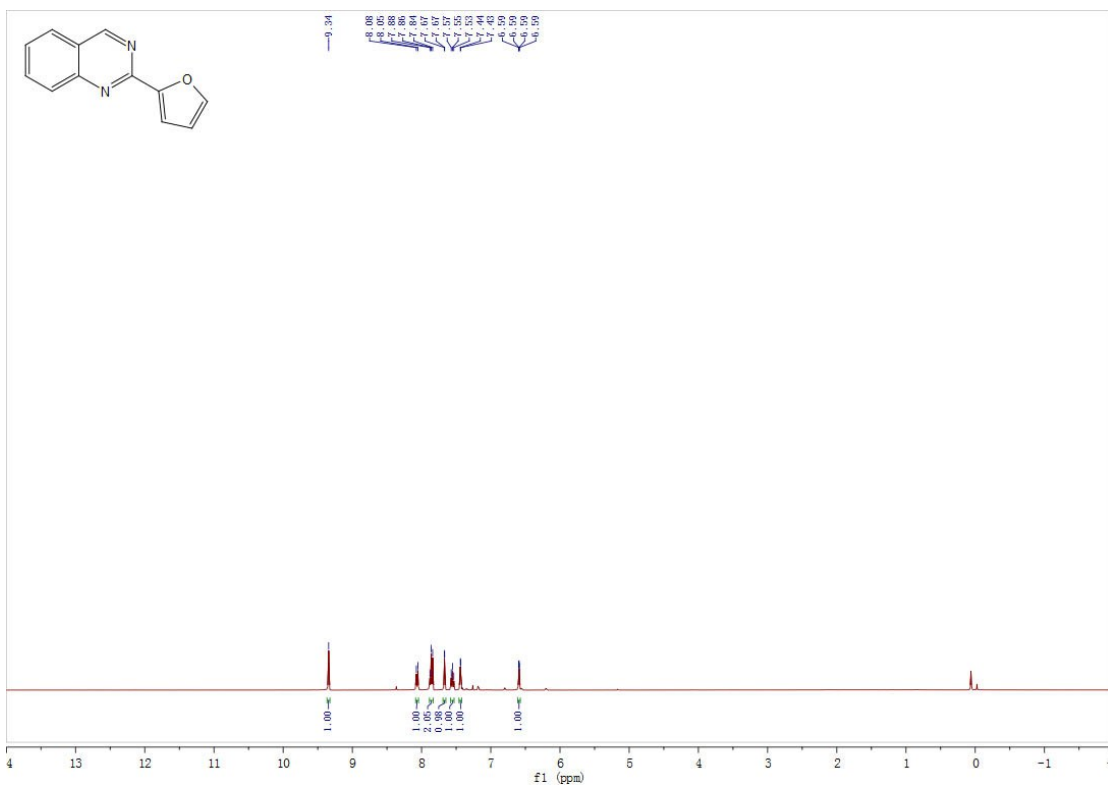
¹³C NMR of 4e



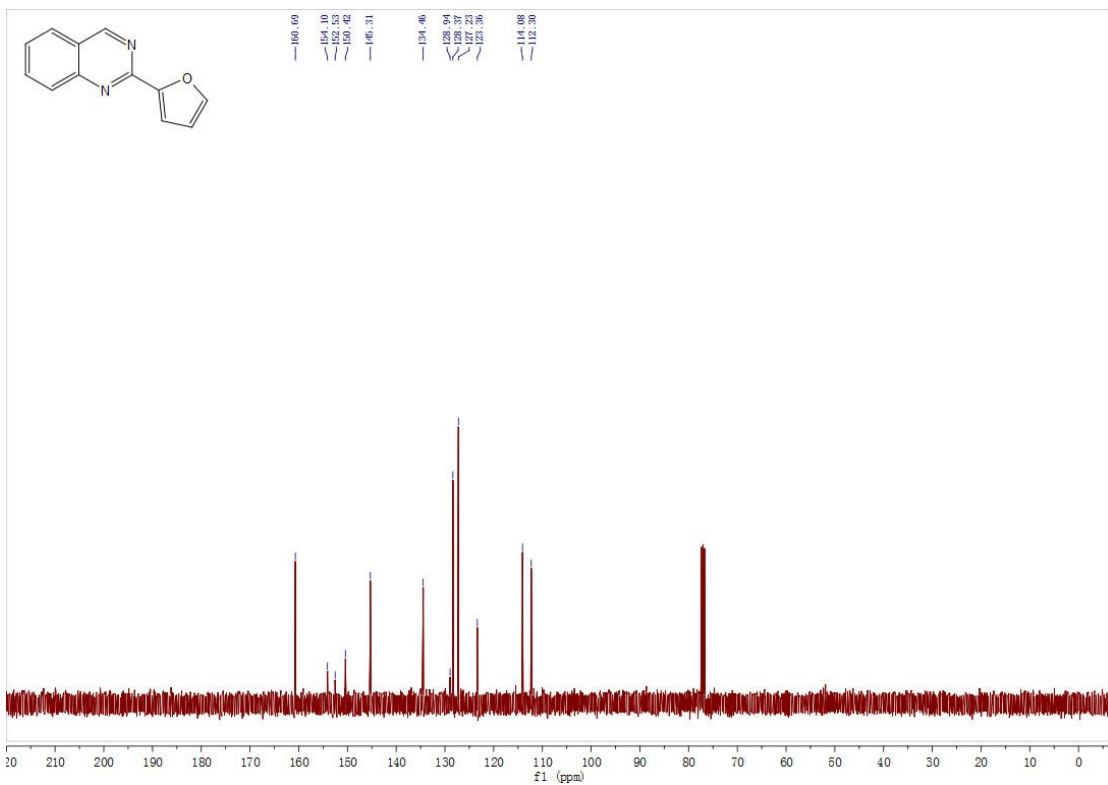
¹H NMR of 4f



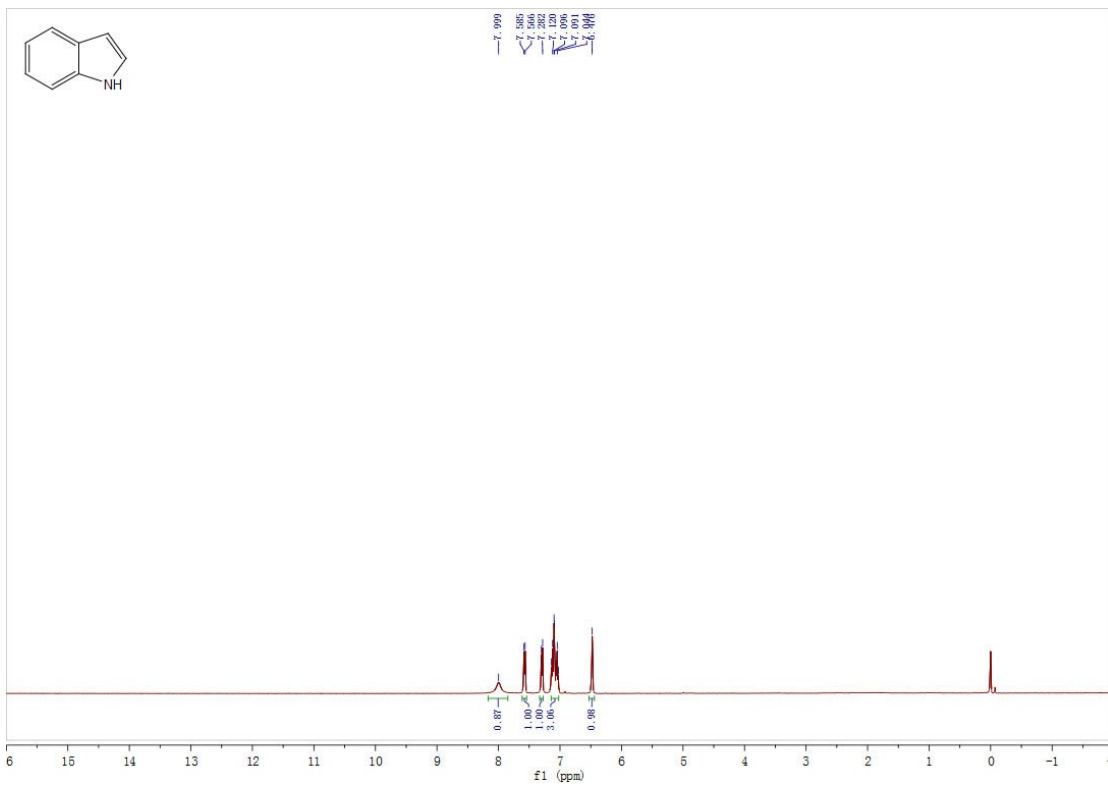
¹³C NMR of 4f



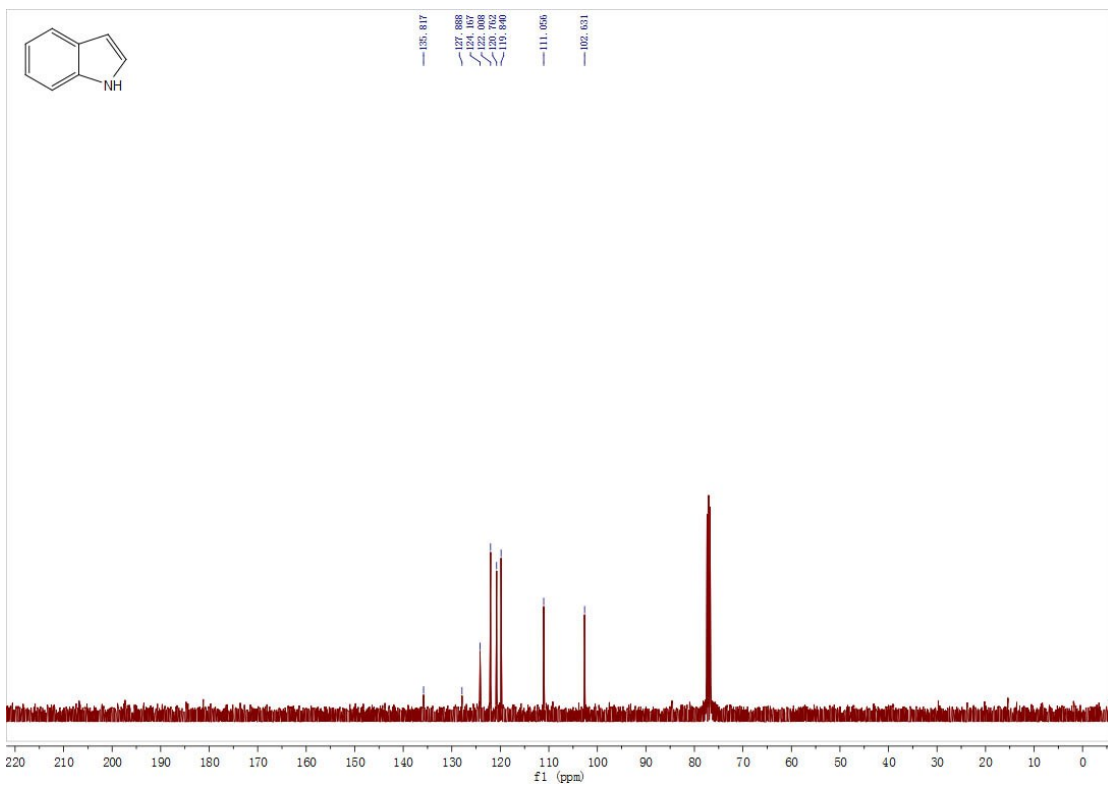
¹H NMR of **4g**



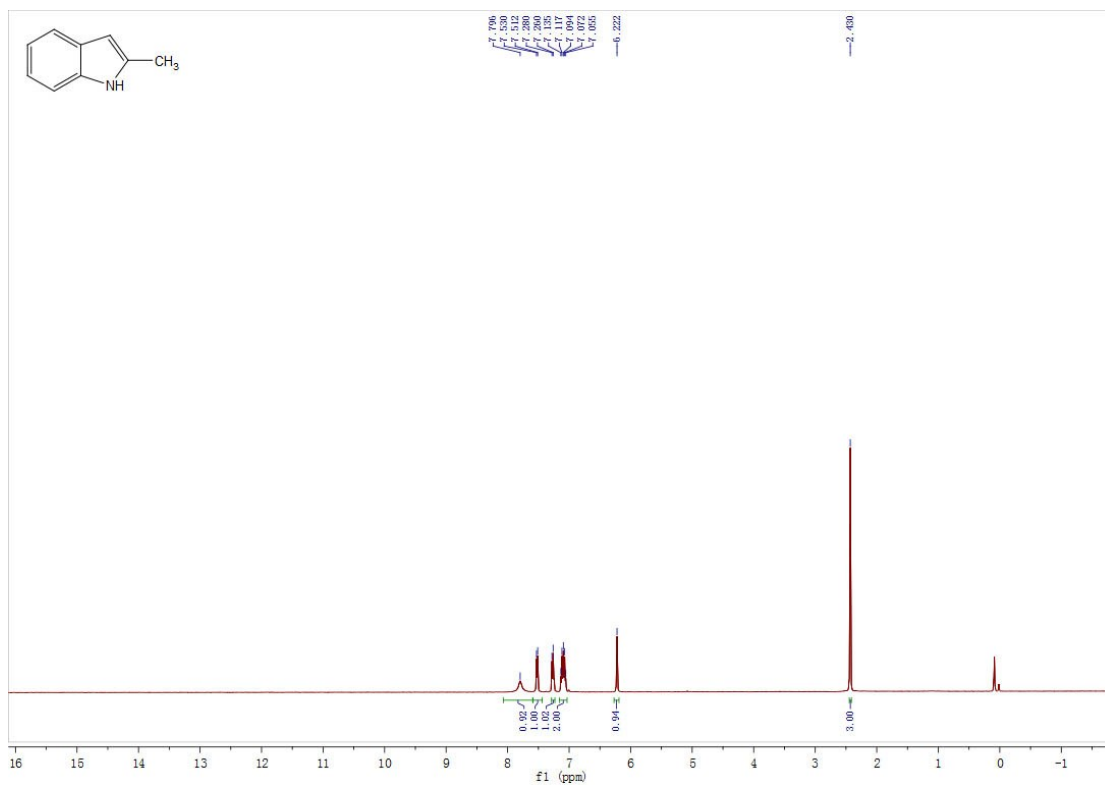
¹³C NMR of **4g**



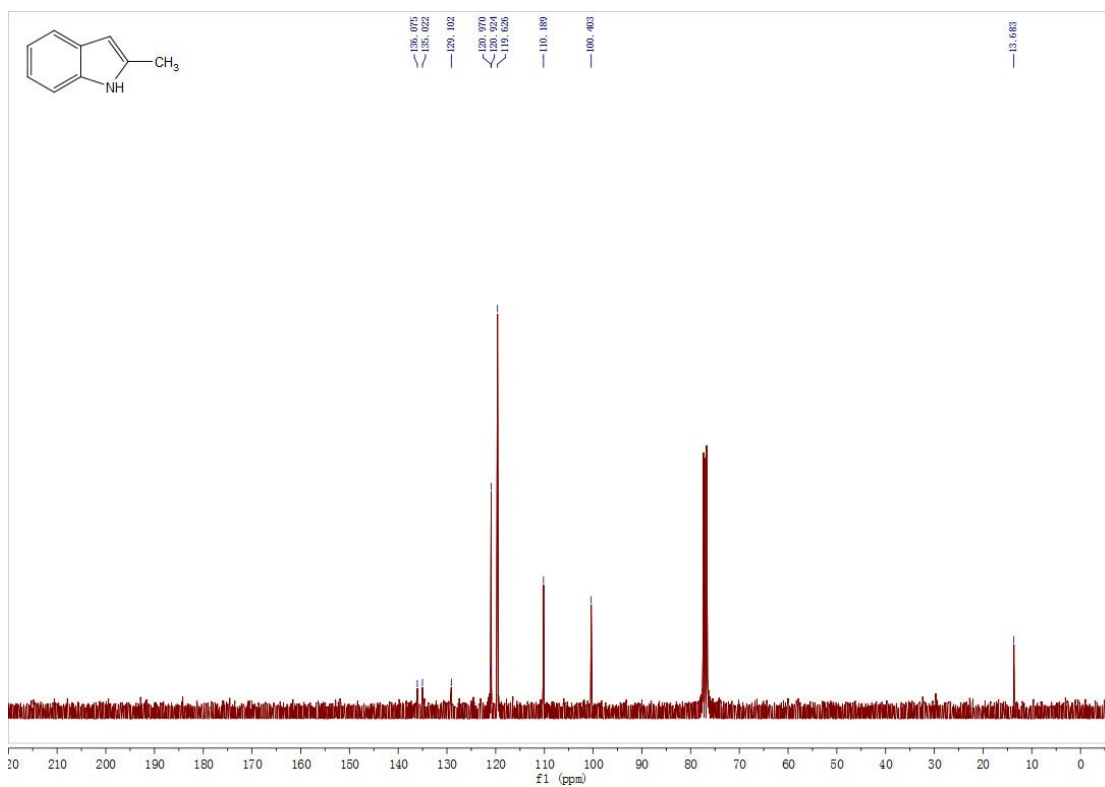
¹H NMR of 4h



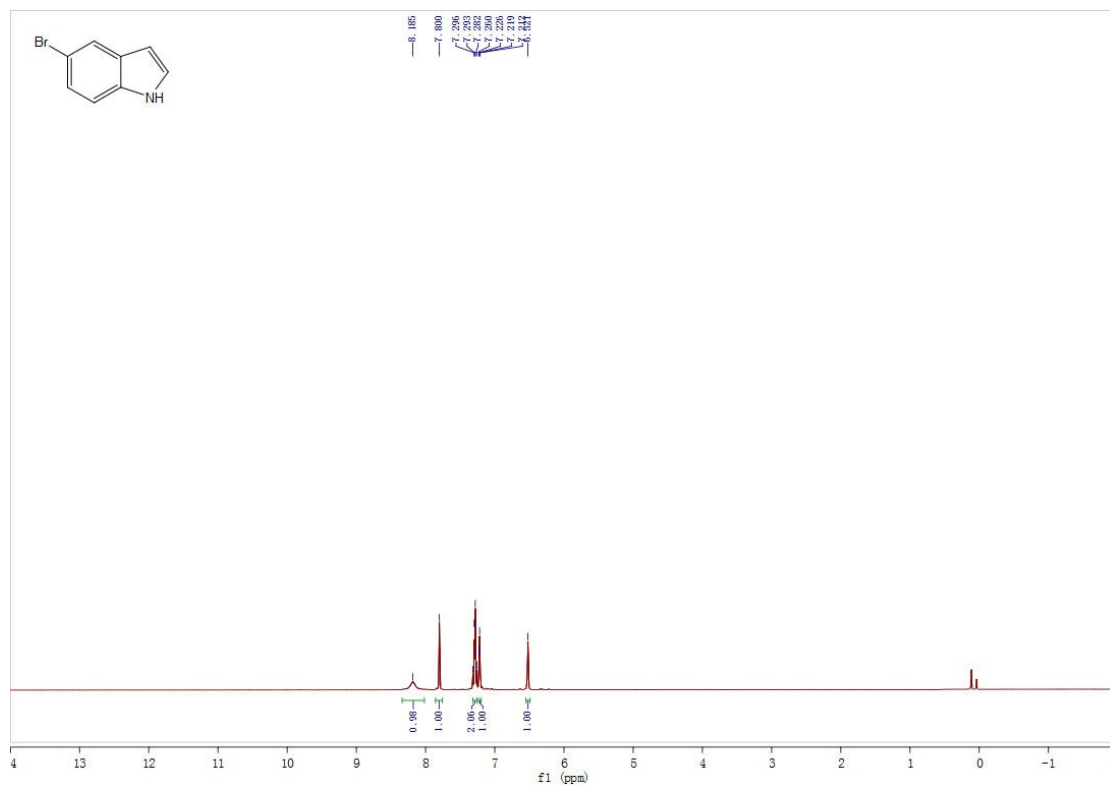
¹³C NMR of 4h



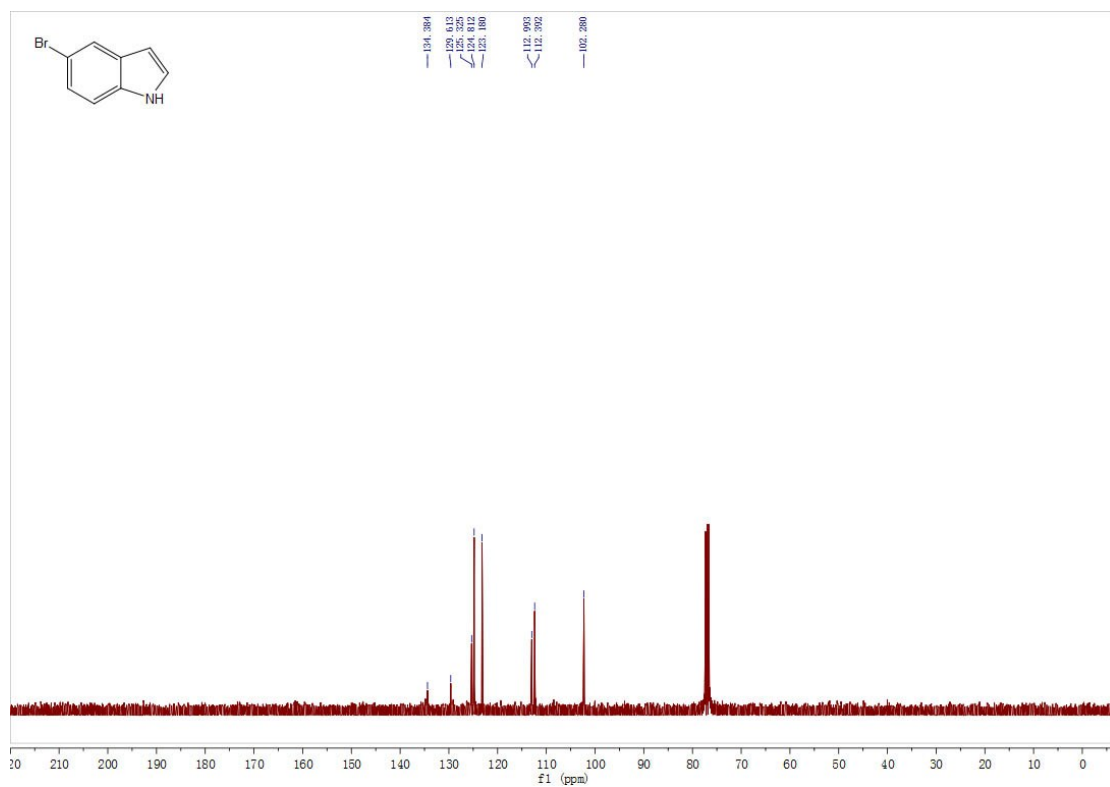
¹H NMR of **4i**



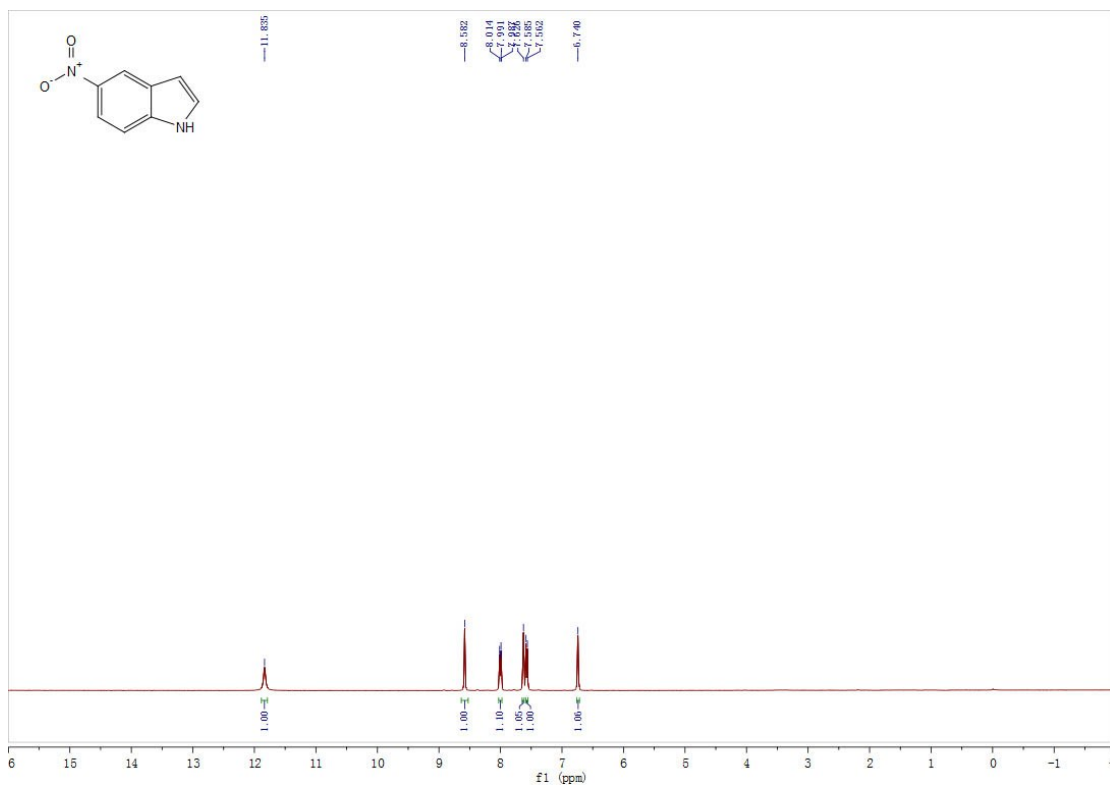
¹³C NMR of **4i**



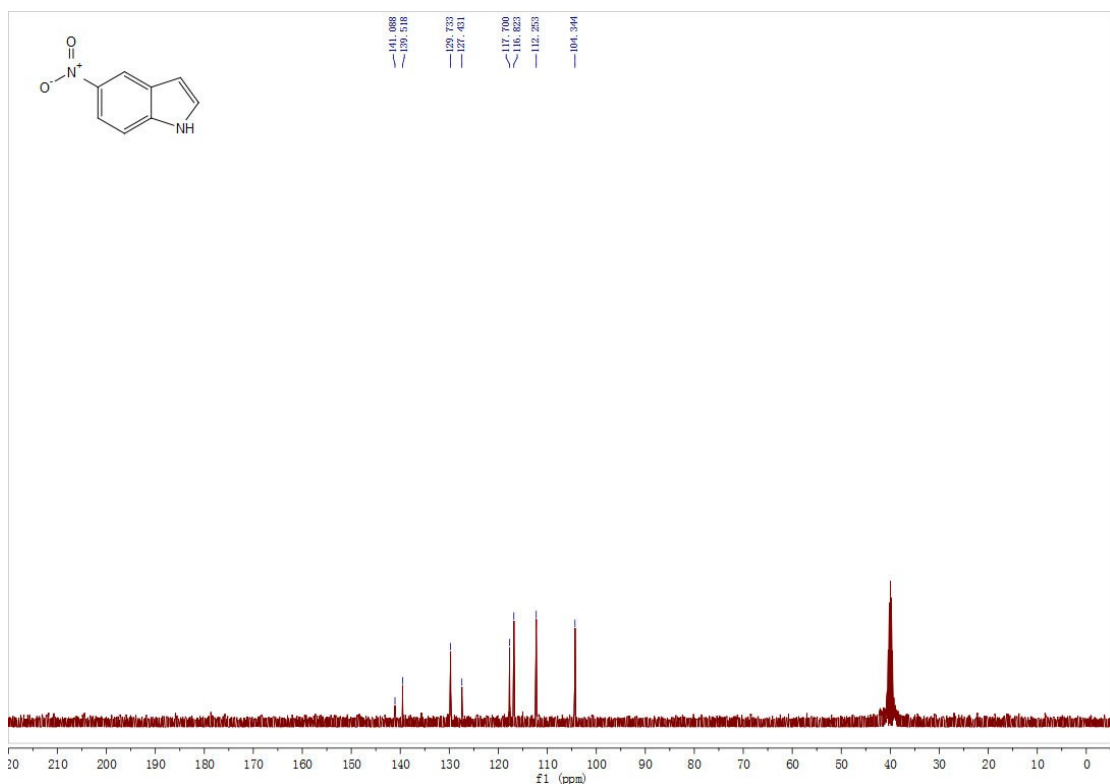
¹H NMR of **4j**



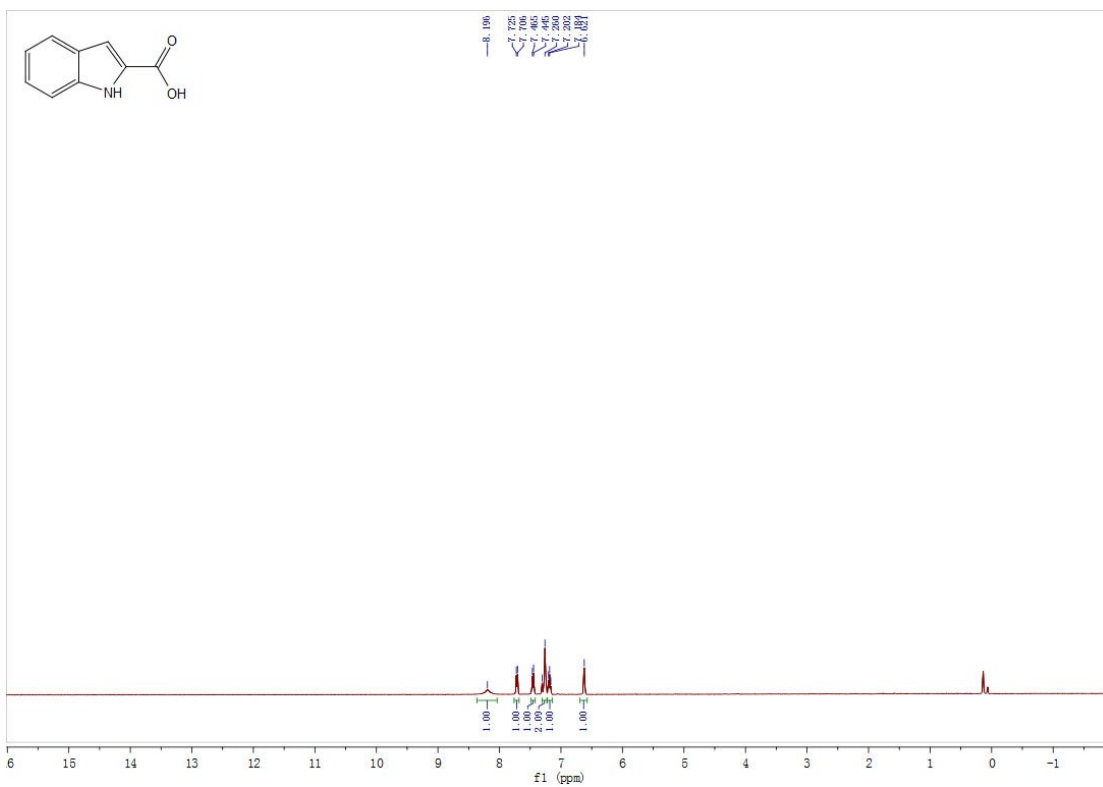
¹³C NMR of **4j**



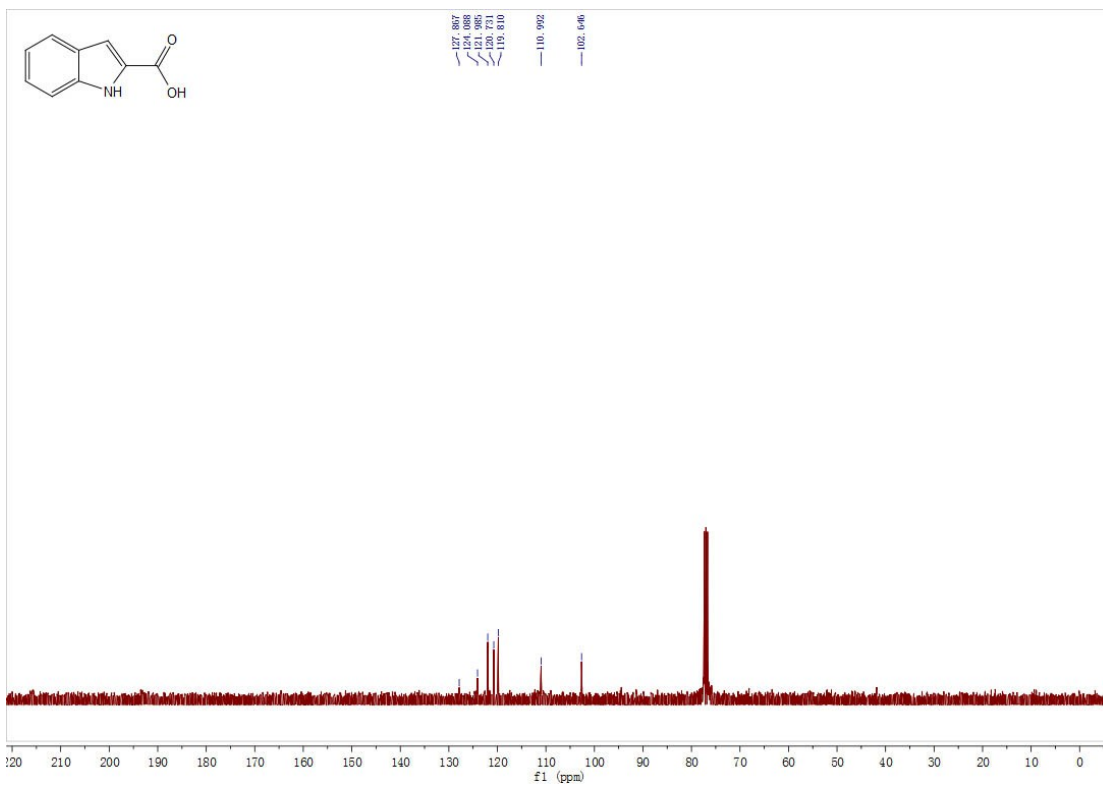
¹H NMR of 4k



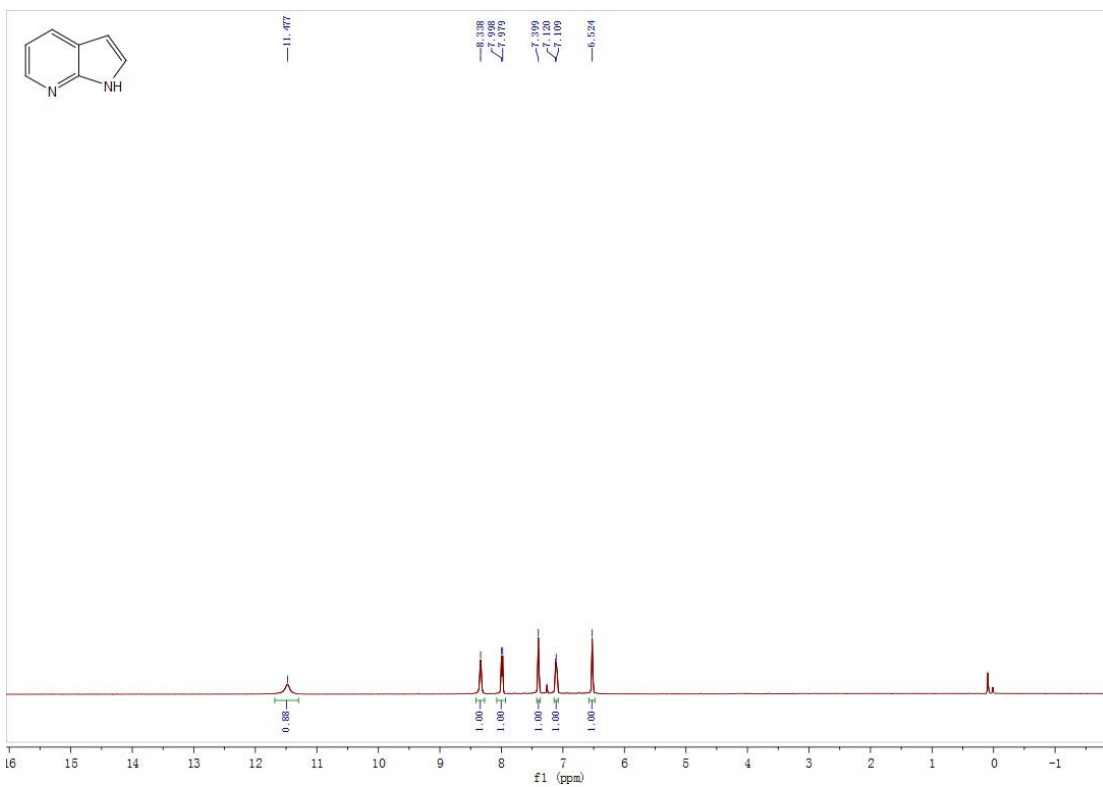
¹³C NMR of 4k



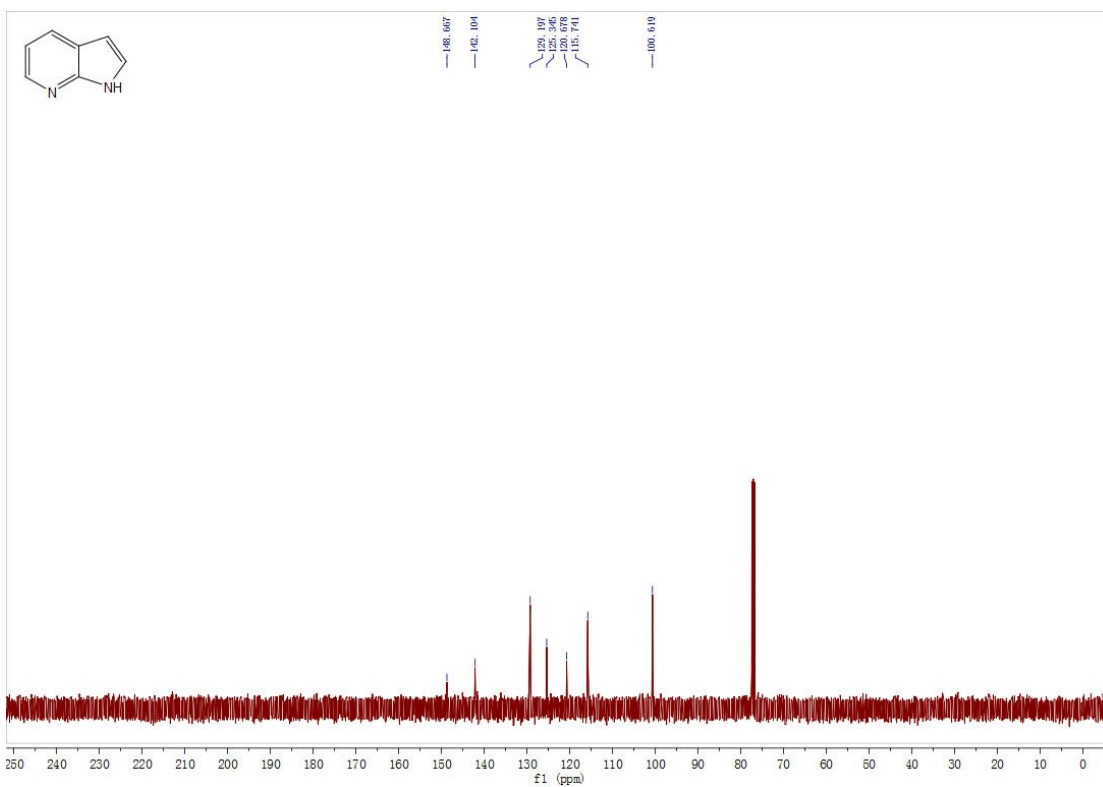
¹H NMR of **4I**



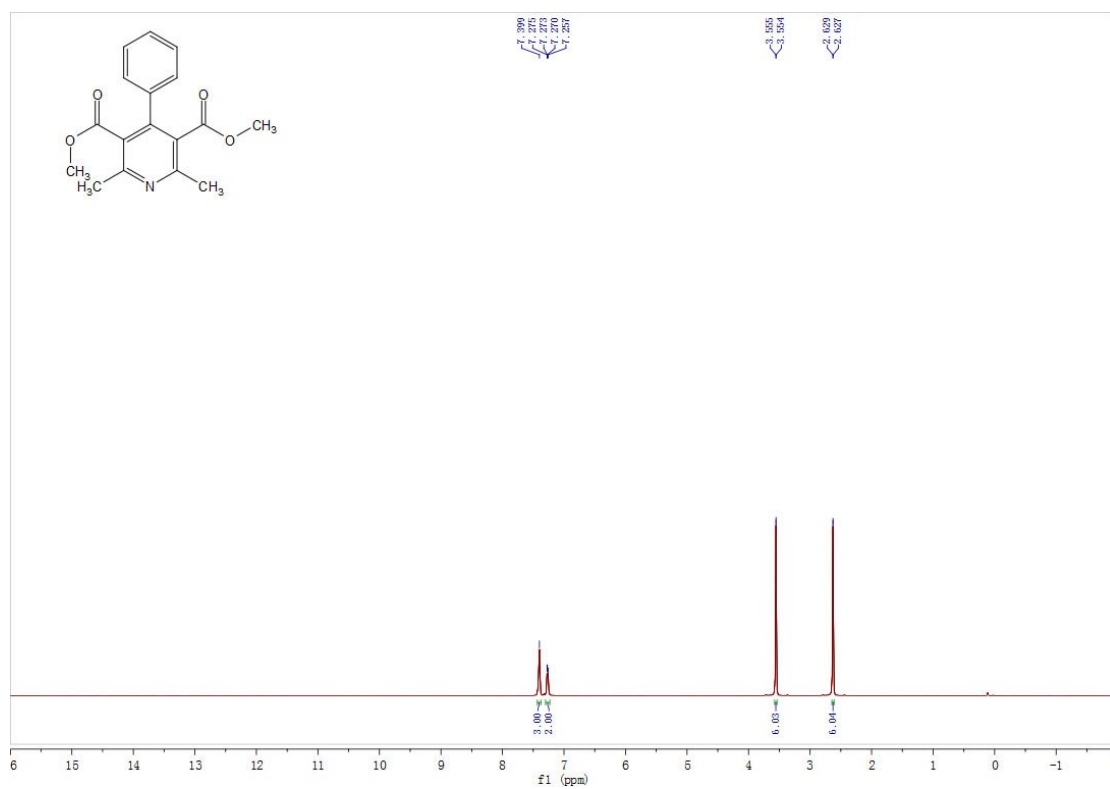
¹³C NMR of **4I**



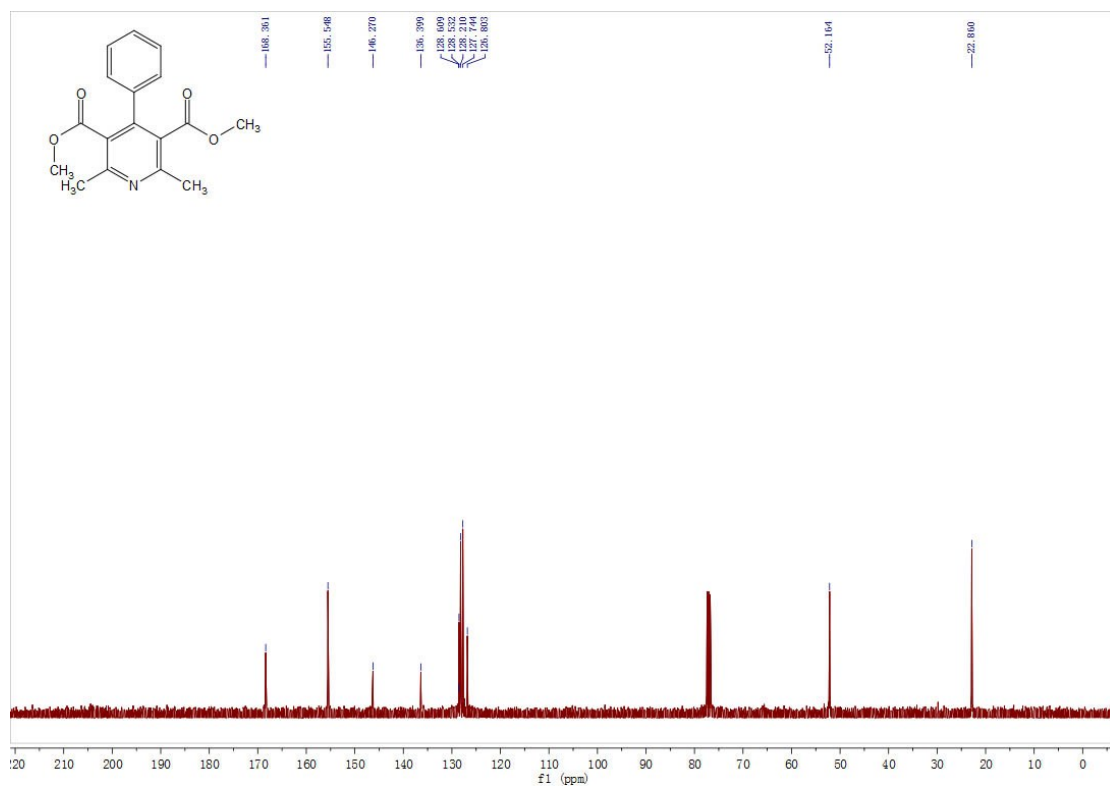
¹H NMR of 4m



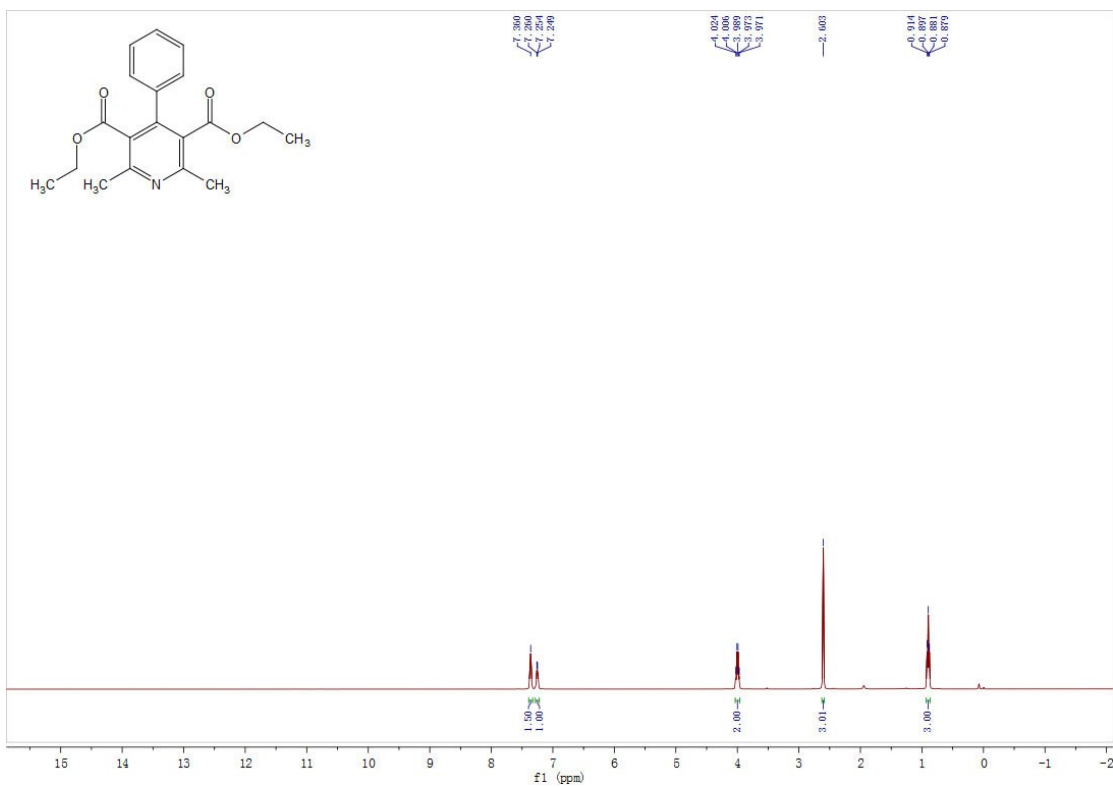
¹³C NMR of 4m



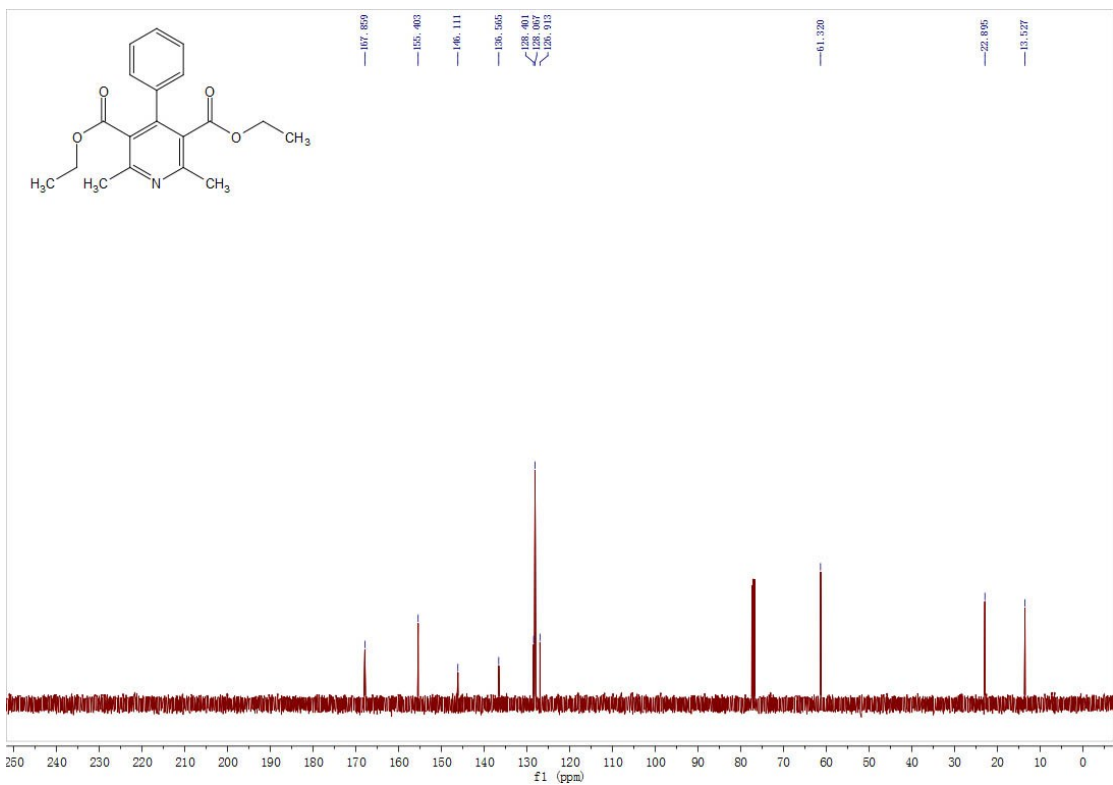
¹H NMR of 4n



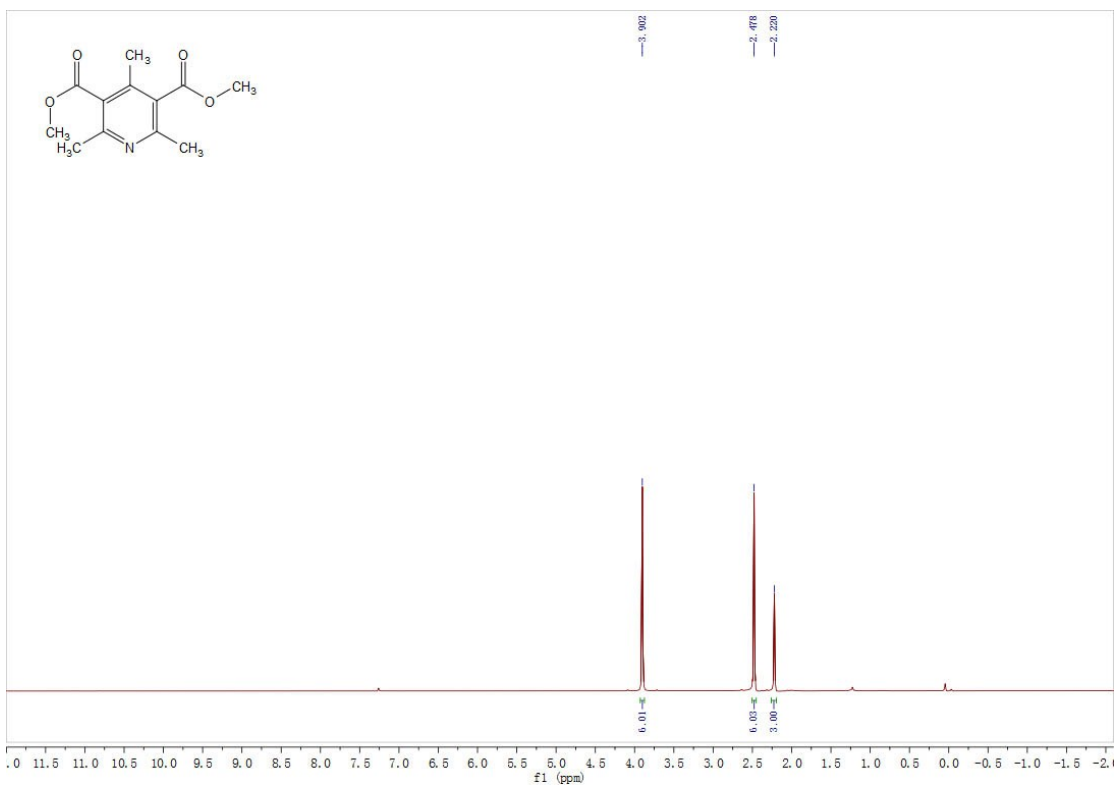
¹³C NMR of 4n



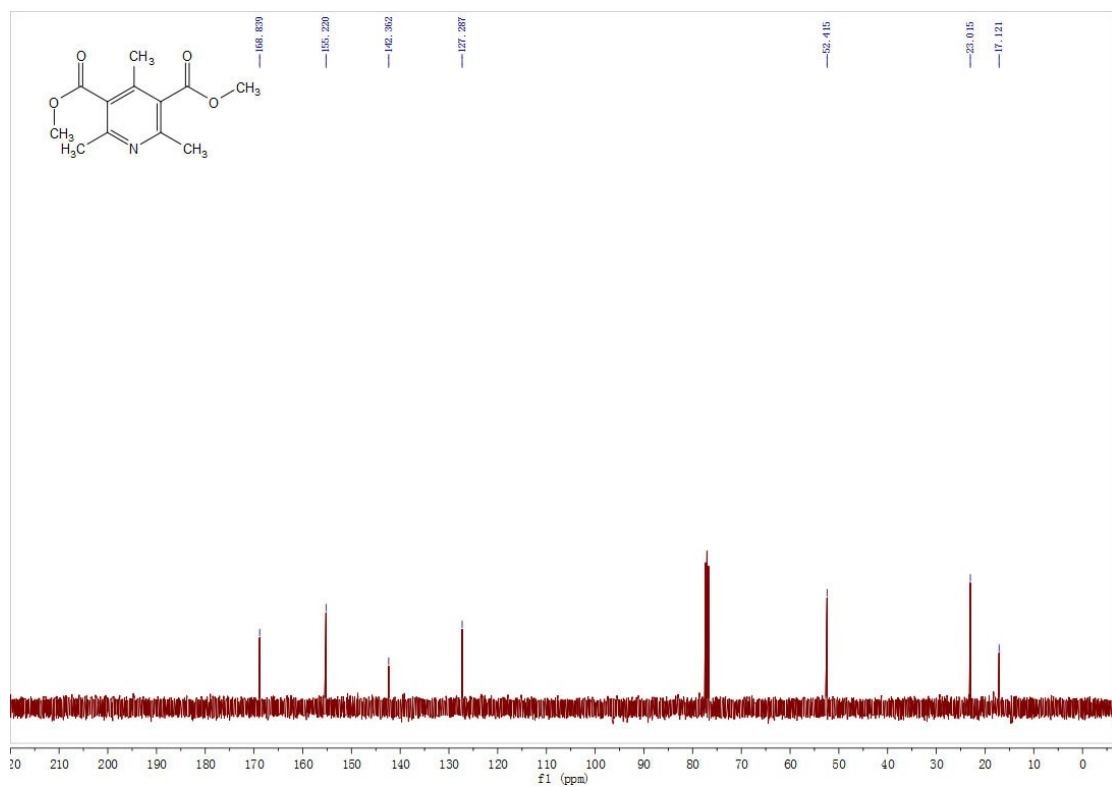
¹H NMR of 4o



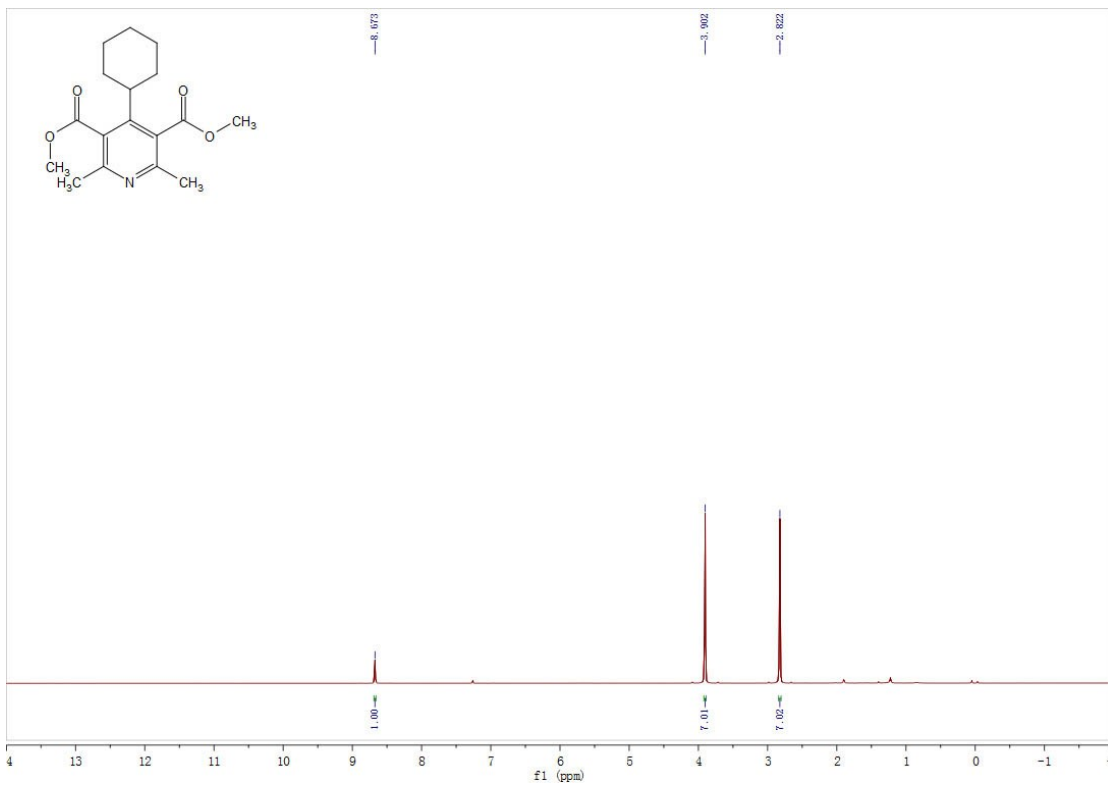
¹³C NMR of 4o



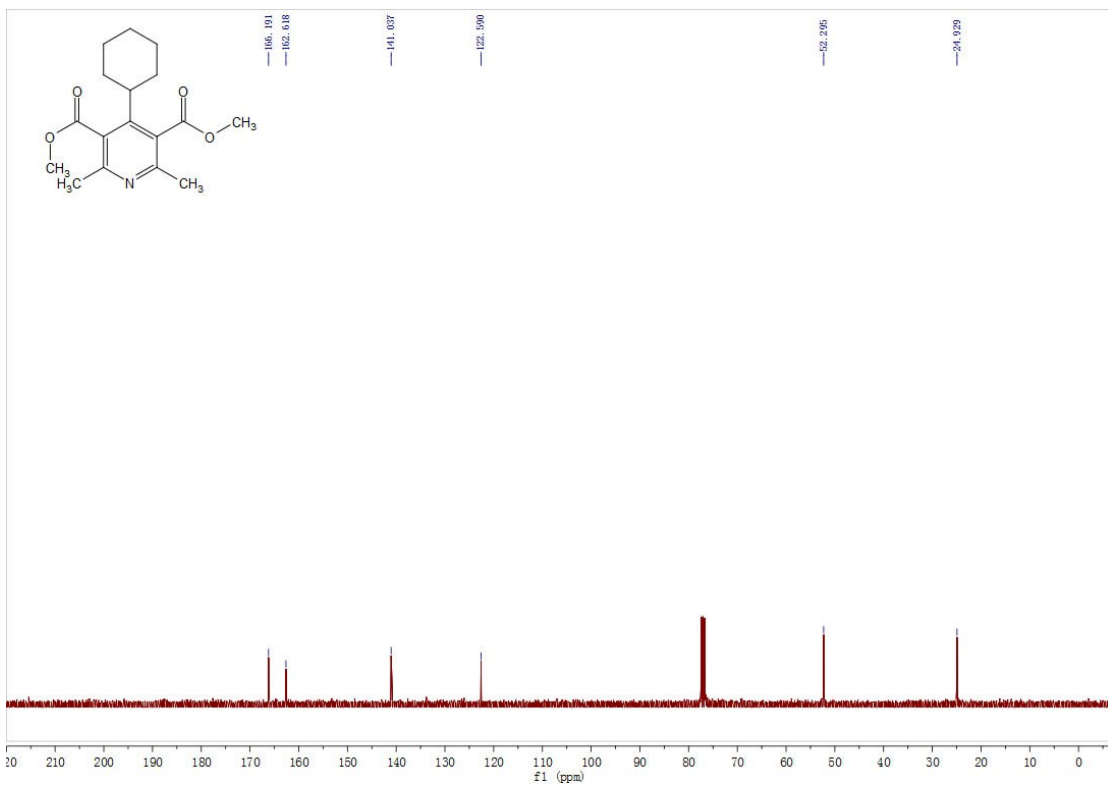
¹H NMR of 4p



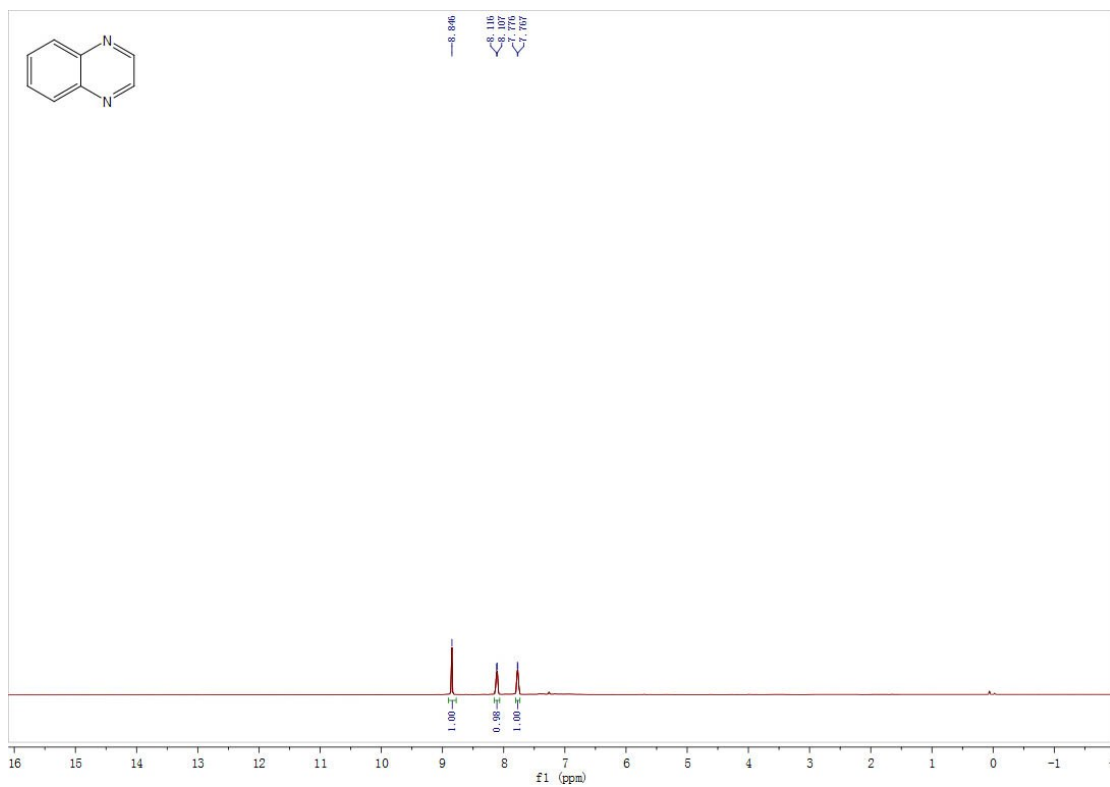
¹³C NMR of 4p



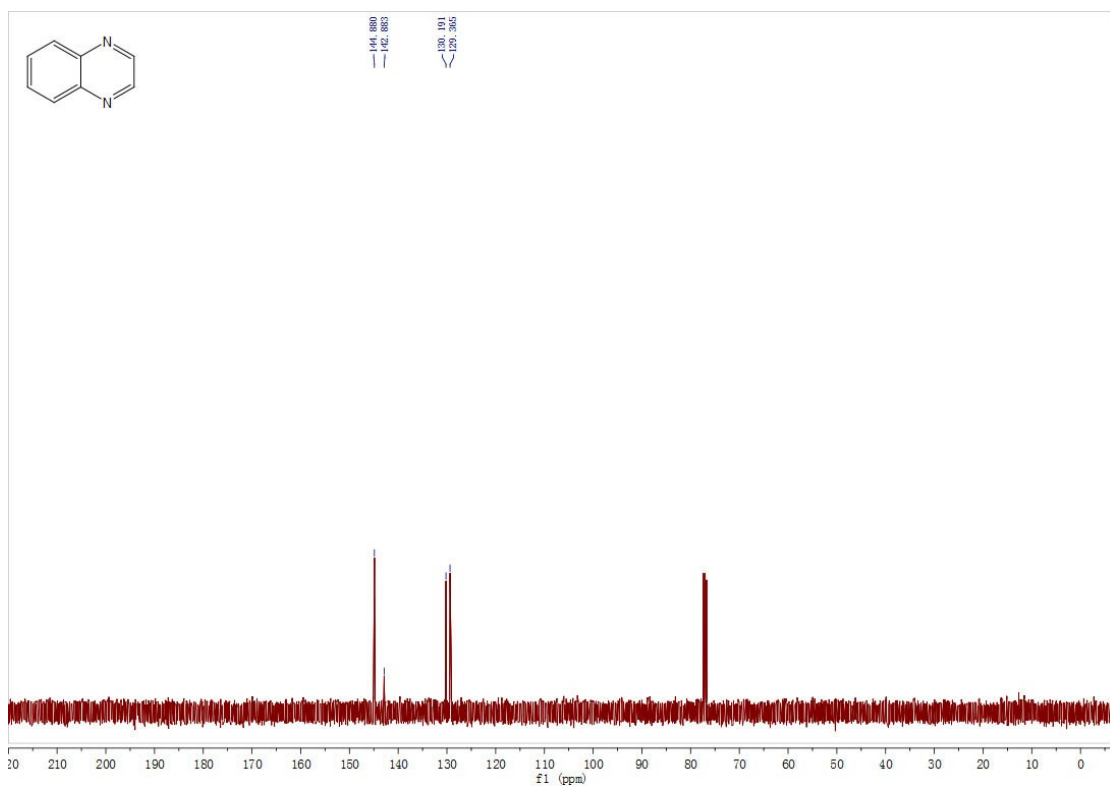
¹H NMR of 4q



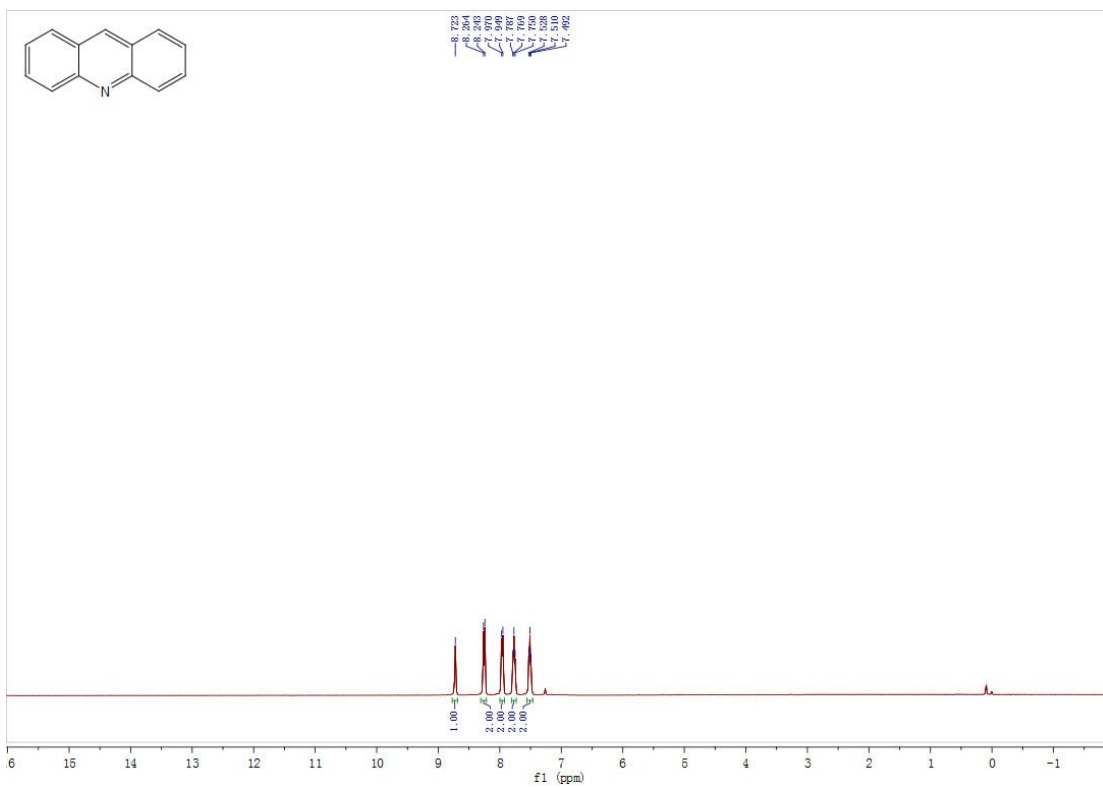
¹³C NMR of 4q



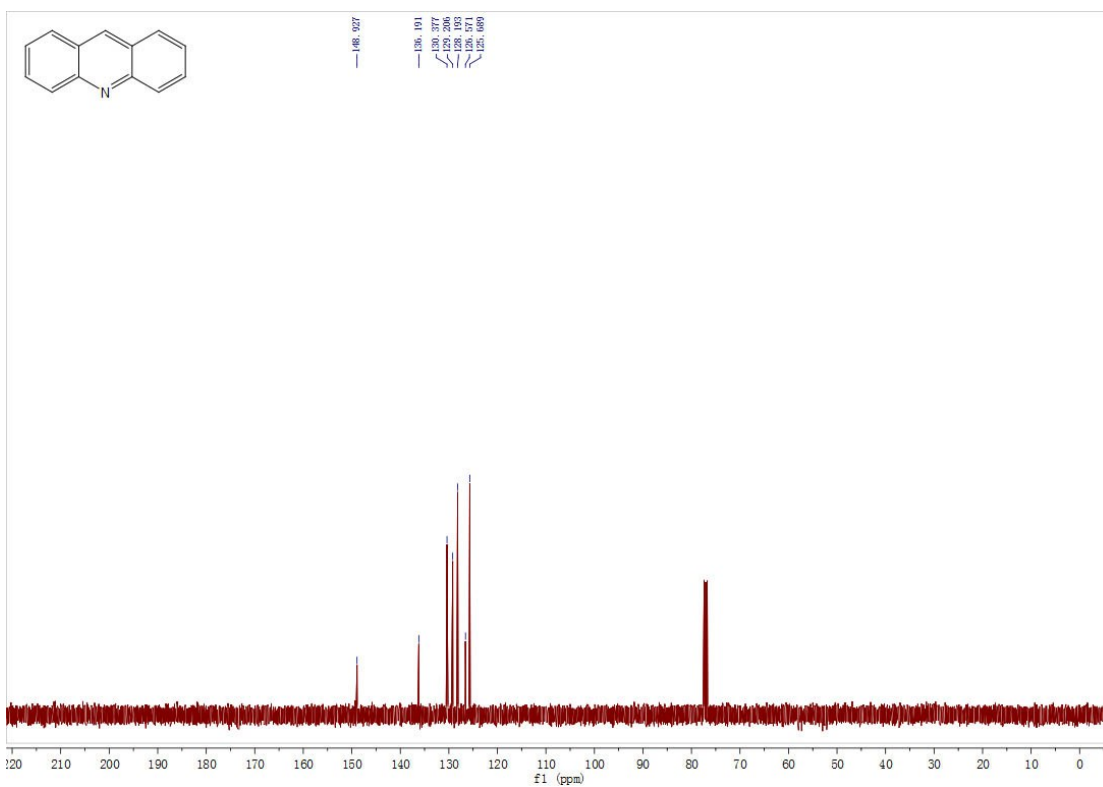
¹H NMR of 4r



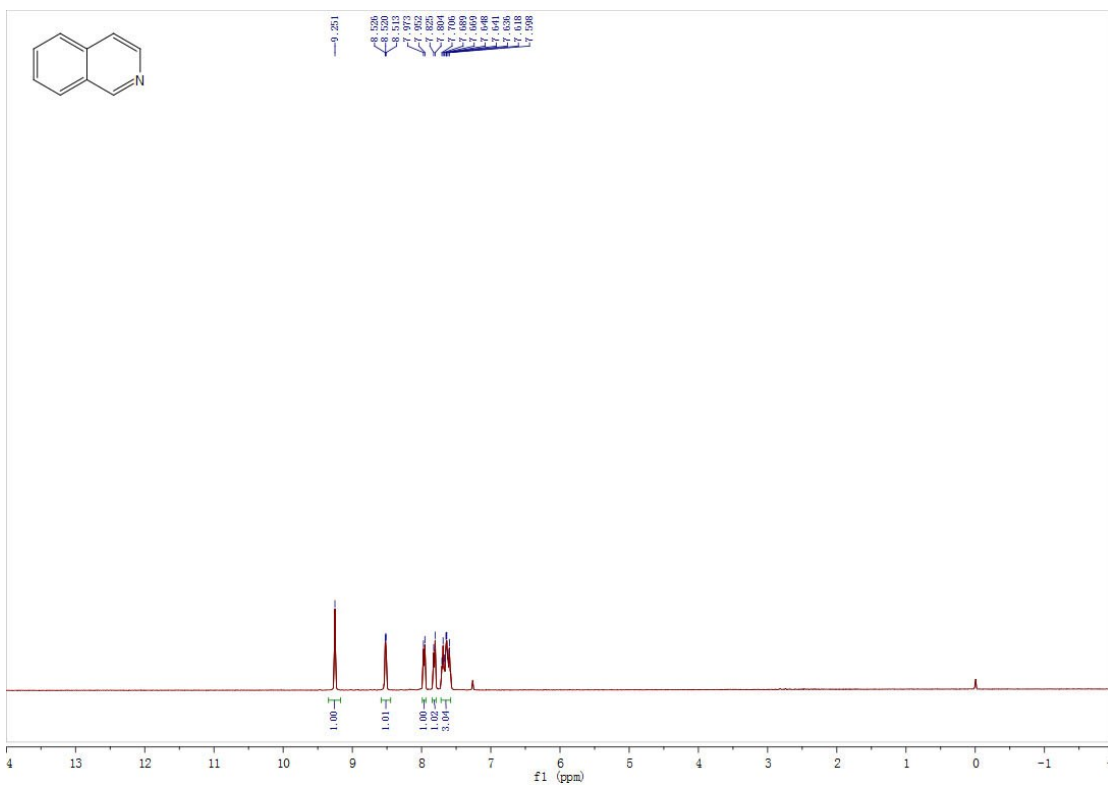
¹³C NMR of 4r



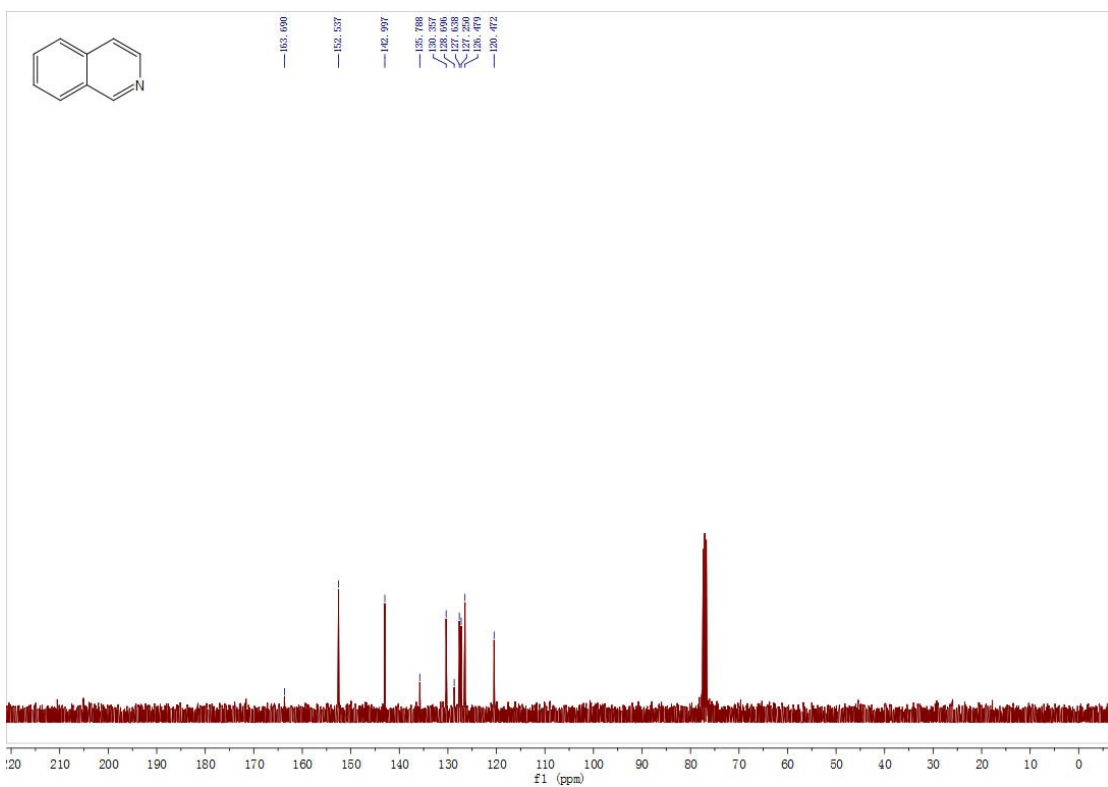
¹H NMR of 4s



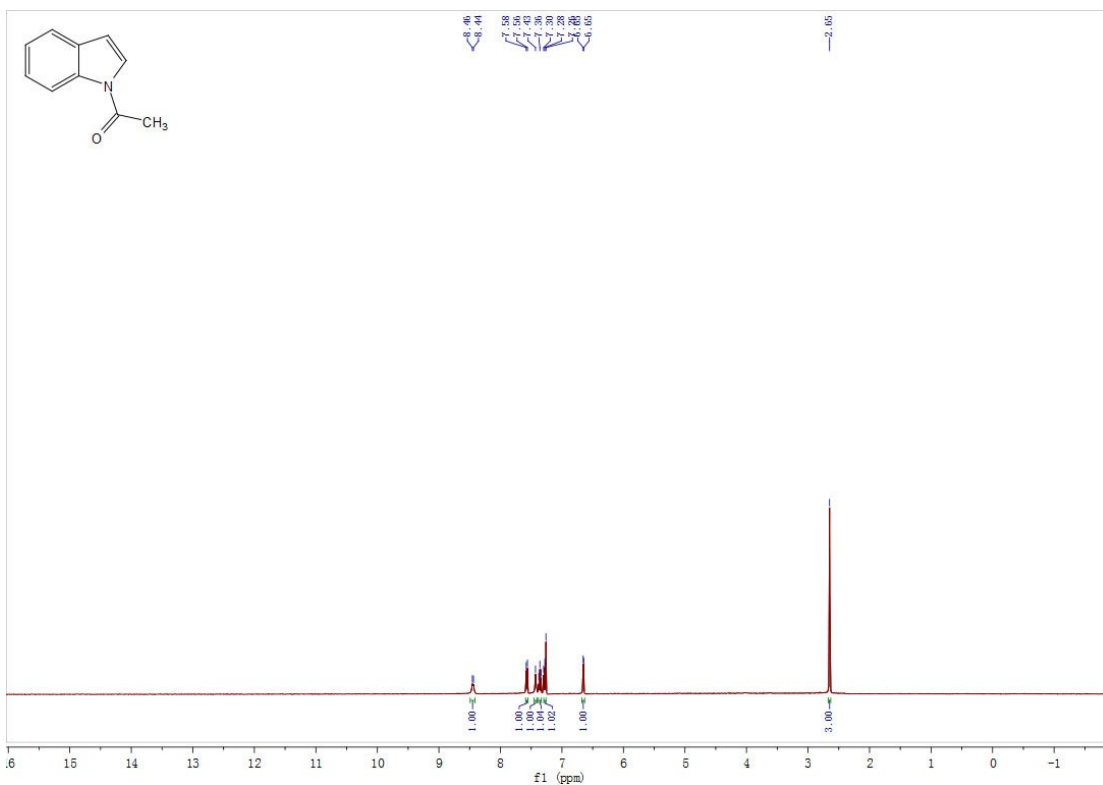
¹³C NMR of 4s



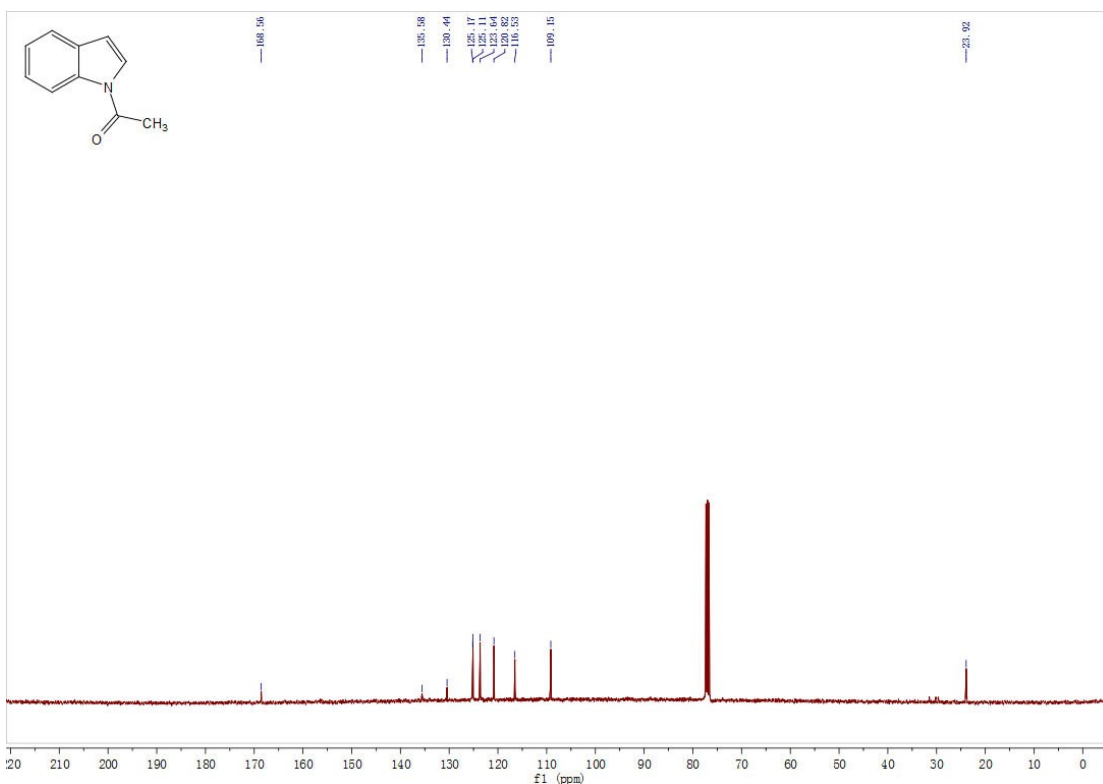
¹H NMR of 4t



¹³C NMR of 4t



¹H NMR of 7b



¹³C NMR of 7b